

INSTITUTO TECNOLÓGICO Y DE ESTUDIOS SUPERIORES DE MONTERREY

CAMPUS MONTERREY

DIVISIÓN DE MECATRÓNICA Y TECNOLOGÍAS DE LA INFORMACIÓN

FEEDBACK SCHEME BASED ON FUZZY CONTROL
AT NANOMETER SCALE



**TECNOLÓGICO
DE MONTERREY®**

THESIS

PRESENTED AS PARTIAL REQUIREMENT
TO OBTAIN THE DEGREE:

MASTER OF SCIENCE IN AUTOMATION

BY:

DIEGO VIDAL ESCAMILLA COLLI

MONTERREY, N.L.

MAY 2011

DEDICATION

To:

God

My family:

My parents: who taught me the value of studying and put in my heart the desire of
being as good as I might be.

My grandparents: they always make me smile and brighten my life.

My sisters: whom I love and appreciate

Grissel: You fill my heart with love.

ACKNOWLEDGMENTS

To my parents, Willie Escamilla and Severeana Collí, thank you for your love, support and comprehension.

To my advisors, Rodolfo Cortés, PhD., and Héctor Siller, PhD., for your teachings, friendship, guidance and help. To my synodals, Federico Guedea, PhD., Víctor Coello, PhD., and Francisco Palomera, PhD., for the revision and comments of this research work.

Special thanks to Ana Laura, Paulina, Israel, César and Lizette for your friendship and all your help.

To my classmates and friends, especially César Cantú and José Luis Guerra, thank you for everything.

ABSTRACT

Fuzzy control is a practical alternative for a variety of challenging control applications, since it provides a convenient method for constructing nonlinear controllers via the use of heuristic information. In this work, it is proposed a control system based on fuzzy logic to control the tip-sample distance in a scanning near field optical microscope (SNOM) using fuzzy control. The fuzzy controller design assumes only one input signal defined as the difference of the sampled signal (tuning fork-tip) and the reference signal, which are compared through designed software. This signal is used as the rule-base of the fuzzy logic controller. It was used LabView 8.2 to develop the set of rules on how to control the process. A basic data acquisition is used as interface to manipulate the fuzzy controller as feedback scheme in the positioning system (piezoelectric bimorph) for the shear force control. The approach curve of the shear-force measurement of the piezoelectric bimorph was obtained using this scheme. In conclusion, this approach can be viewed as simple and reliable as feedback scheme based on fuzzy control for shear force control in a SNOM. However, in many cases, the fuzzy control can be used to improve existing traditional controller systems by adding an extra layer of intelligence to the current control method.

CONTENT

1	PRESENTATION	7
1.1.	INTRODUCTION	7
1.2.	MOTIVATION AND JUSTIFICATION	8
1.3.	LITERATURE REVIEW	9
1.4.	OBJECTIVES	11
2	THEORETICAL FRAMEWORK	12
2.1.	SHEAR FORCE TECHNIQUE.....	12
2.2.	QUARTZ TUNING FORK.....	19
2.3.	FUZZY CONTROL	22
3	EXPERIMENTATION.....	32
3.1.	SCHEMATIC SYSTEM.....	32
3.2.	CALIBRATION	35
3.3.	CONTROL PANEL	39
3.4.	FUZZY CONTROL STRATEGY DESIGN.....	41
3.5.	EXPERIMENTAL RESULTS.....	46
4	CONCLUSIONS	37
4.1.	CONCLUSIONS	51
4.2.	CONTRIBUTION.....	52
4.3.	FUTURE WORK.....	52
5	REFERENCES.....	54
6	APPENDIX A MORPHOLOGIC MATRIX EXTENDED.....	56
7	APPENDIX B SOFTWARE DESCRIPTION.....	61

1 PRESENTATION

1.1. Introduction

The scanning near-field optical microscope (SNOM) is an microscope used to obtain resolution beyond the diffraction limit and it has overcome the resolution limit of classical optical microscopy [1,2]. The acronym for SNOM [3] was appointed by Pohl and his research team. An essential requirement in the SNOM is to obtain high resolution images. In this case, tip must be carried and maintained at a constant distance between the tip and the sample [4]. According to this, many alternatives have been proposed to regulate the tip-sample gap to allow to provide a constant distance sampling and then, the possibility to obtain additional information about sample topography. Non-contact atomic force microscope is an attractive option to solve this problem, especially if the sample is sensitive enough to have non-contact with the probe in order to not damage either the tip or the sample, but this alternative is difficult to implement using conventional optical fiber probes. Nevertheless there are cases where this has been implemented using a sharp probe in a way that resembles a conventional atomic force microscope (AFM) cantilever [5]. Anyway, the shear force technique (SFT) [6,7] is a strategy that has proven to be a convenient option to establish a mechanism for feedback control distance between a probe scanning and a sample surface. The most widespread method has been proposed simultaneously by Betzig *et al* [6] and by Toledo-Crow *et al* [7]. In both cases the amplitude detection is based on optical means [8,9], they require dedicated laser whose beam has to be suitable readjusted after each fiber replacement in order to sense the optical signal on probe tip. However, the optical method used to detect the shear force can cause problems when imaging photosensitive materials. Moreover, it is probably that stray light can perturb detection of the generally weak optical signal.

1.2. Motivation and Justification

The manipulation system is based on the use of piezoelectric bimorph and due to the nonlinearity characteristics of these actuators [19]; we propose the use of fuzzy logic control, in order to provide robustness to the tuning fork-piezoelectric controller system. In general, the proportional-integral control strategy in shear force distance control is commonly used. Grober *et. al.*[20] showed that conventional proportional and integral (PI) feedback control is a good option for most uses of tuning forks, comparing the response of feedback loop with open loop resonator one. Although the PI offers a quick response control in general, for high resolution imaging, it is necessary improve the scanning rate. Most strategies to get this resolution have been focused on the modification of tuning fork features like Q-factor [21] instead of controller design. In this work it is proposed a shear force control mechanism based on a fuzzy control design, using tuning fork as sensor and a piezoelectric bimorph as actuator in order to reduce the effect of non-linearity of piezoelectric bimorphs.

At present, the development of new technologies in several fields, has a tendency to produce smaller and more compact devices, such as BioMEMS, because of this situation there is a need to sense, measure and inspect these devices. In this way, particularly image-forming systems such as the microscope or profilometers, which allow the reconstruction of the surface of an object with a resolution of the order of nanometers, are increasingly required. SNOM is a system that provides this possibility because of their capabilities mentioned above. Moreover, it is important to mention that in Mexico the number of researchers working in the area of optical near-field is very small, so that, this work offers the opportunity to represent an instrumentation of collaboration.

1.3. Literature Review

In the literature review made it for this research were found it two areas of opportunity to bring: The type of control used, which have been tested only with Proportional-Integral controllers and how to implement the sensing system using a tuning fork. In Appendix A the morphologic matrix is extended and summaries of each of the studies reviewed.

Table 1. Literature review morphologic matrix

Research Work	Control Strategy	Sensing	Arrangement
Leong <i>et al</i> (1995)	None	Capacitive	Parallel
Walid <i>et al</i> (1996)	None		Parallel
Salvi <i>et al</i> (1997)	None	Current-voltage Tuning fork	Prongs
Karrai <i>et al</i> (2000)	Proportional-Integral	Current-voltage Tuning fork	Parallel
Grober <i>et al</i> (2000)	Proportional-Integral	Current-voltage Tuning fork	Parallel
Ohkub <i>et al</i> (2003)	Proportional-Integral	Interferometry and Current-voltage Tuning fork	Prongs
Gucciardi <i>et al</i> (2005)	None	Interferometry	Perpendicular
Escamilla <i>et al</i> (2011)	Fuzzy control	Current-voltage Tuning fork	Perpendicular

It can be concluded that the previous work researches have been focused on physical techniques to get a higher resolution in the scanning process by shear forces; nevertheless, in this work fuzzy logic control is proposed to be used to improve the distance control for a shear force technique and in a future work, to obtain a higher resolution. On the other hand, there are several kinds of mechanical arrangement to use

a tuning fork piezoelectric as a sensing dispositive. Figure 1 shows the three main techniques used and the chosen one to sense the shear forces.

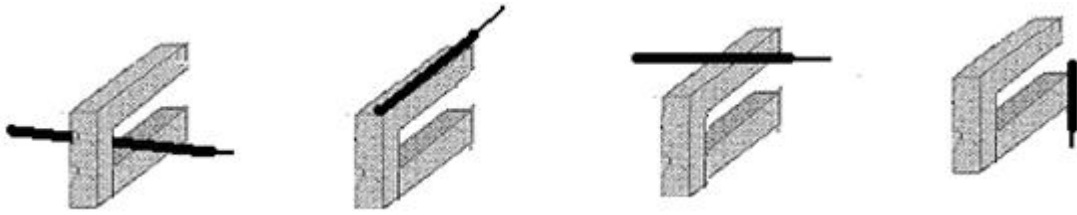


Figure 2. Literature review morphologic matrix

1.4. Objectives

For this thesis the main objectives are:

- 1.-Use the shear force physical phenomena and electronic instrumentation for function and operation of a sensing process surfaces by shear force technique.
- 2.-Design and carry out the instrumentation necessary to perform the sensing and control using the resources available in the laboratory at CICESE.
- 3.-Characterize tuning fork and calibrate the actuators to be used in the process.
- 4.-Develop a LabVIEW based virtual interface for configuration and control of the profile sampling system.
- 5.- Design and implement a fuzzy controller to control a piezoelectric bimorph actuator in order to maintain a constant distance between the fiber tip and the sample sensing to obtain information from the scanned profile of the particle.

2 THEORETICAL FRAMEWORK

2.1. Shear Force Technique

Shear force technique (SFT) is a technique that consists of a fiber that maintains a constant amplitude vibration through a control mechanism. Here a tip-probe is oriented perpendicular to sample as it approaches to the surface, typically it vibrates laterally at one of its fundamental mechanical resonance mode in the range of 10-100 KHz. The vibration is reduced due to presence of shear forces.

The tip presents a behavior where the tip oscillation signal shows a damping tendency as the tip approaches to surface. In particular when the tip almost touches the surface the amplitude signal decreases in a drastically way. Furthermore, a dither piezo is used to drive the probe at one of its resonances, applying a small AC voltage and very small forces causes the damping effect [6]. The origin of these small forces, that cause this feature, is so far not entirely clearly defined. There are several proposals that attempt to explain the origin of the physical phenomenon, the attenuation of a vibrating probe when approaching a surface at a nanometer scale, can be explained with the Van der Waals forces and capillary forces [7]. These shear forces reduce the amplitude of the tip vibration and modulation and the characterization of this feature allows designing the control strategy to regulate the position of the tip-sample. The idea is to locate a reference point to compare the current distance from the reference point against previously established and depending on the signal variations is obtained the morphology information of the sample surface. The change through a manipulation of control is directly proportional to the magnitude of the variation of the distance probe-sample.

Once it has shown the physical phenomenon in the sensing system, is important to note that the vibration of the fiber is usually done through a piezoelectric, capable of transforming electrical energy into mechanical energy. As mentioned above, initially the optical methods were used to detect shear forces and feedback, but through the development and continuous improvement in measurement techniques, we began a transition to non-optical methods of measurement because optical methods were

susceptible to external noise. According to Karrai *et. al.* [22] piezoelectric tuning forks are measuring instruments that have been successfully implemented in force detection schemes for scanning probe microscopy applications. Grober *et. al.* [20] proposed a mechanical arrangement based on a parallel probe glued to a tuning fork, see Figure 2.

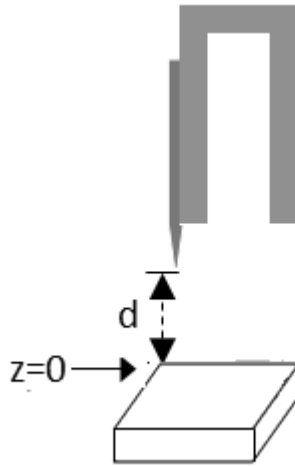


Figure 2. Schematic of shear force technique based on a vibrating fiber.

The shear force distance control method belongs to the electronic detection: the dithering is generated by a piezoelectric element and the perturbation due to the tip-sample distance variations is measured the variation produced, optical or mechanical. Different configurations have been already proposed to measure the shear forces and the tendency is to use a piezoelectric element playing the role of excitation. Table 1 shows that the tip damping generally is measured by sensing changes in capacitance of an electrodes pair or the voltage induced in a piezoelectric element (tuning fork) glued onto the fiber [14], which is a very sensitive method and leads to excellent results [23]. Nonetheless, the tedious and critical gluing of the fragile tuning fork against the fiber is one severe limitation because the sensitive (Q factor) of tuning fork is strongly glue dependent and there is the possibility to degrade it by the migration of the glue along the arms of the fork [24].

Salvi *et. al.* [24], proposed the use of a tuning as a vibrating device in order to move the probe and detect the damping forces in a particular way, consisting in place the probe in middle of the tuning fork. I decided to use a similar mechanical arrangement, but it was not possible to achieve a suitable coupling for sensing changes in our particular measurement system, then, after doing some tests it was decided to use a set up based on a perpendicular design between probe and tuning fork, where a little glue is used to hold the vibration movement, this was decided because it was not possible to implement a suitable holding technique to hold the fiber firmly as Salvi *et. al.*[25] did it. Figure 3 shows the Salvi's proposal.

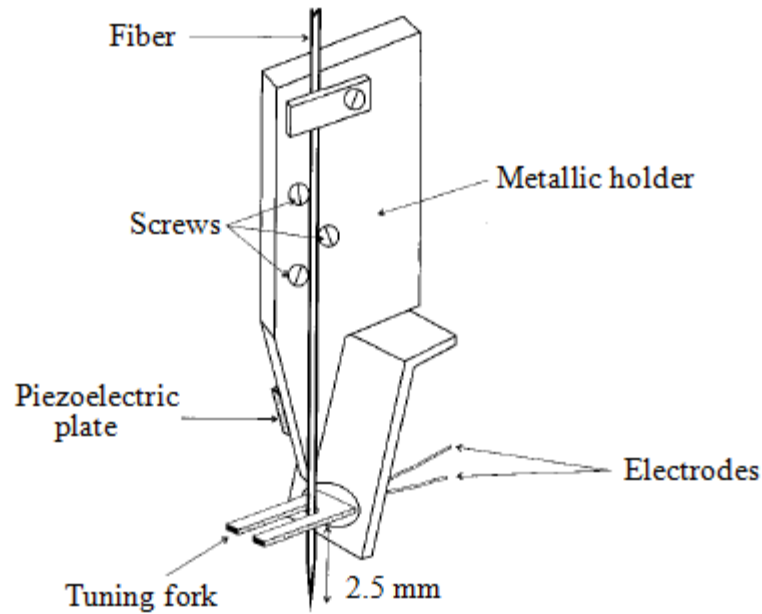


Figure 3. Schematic of the tuning fork and fiber arrangement (prongs).

The variant proposed by Salvi *et. al* [24], works around the gluing problem, so that, the fiber is merely introduced between the two prongs of the tuning fork and held against the prong's junction.

Finally, they show two classical approach curves for tuning fork, using an optical detection and the electronic proposal by them (see Figure 4).

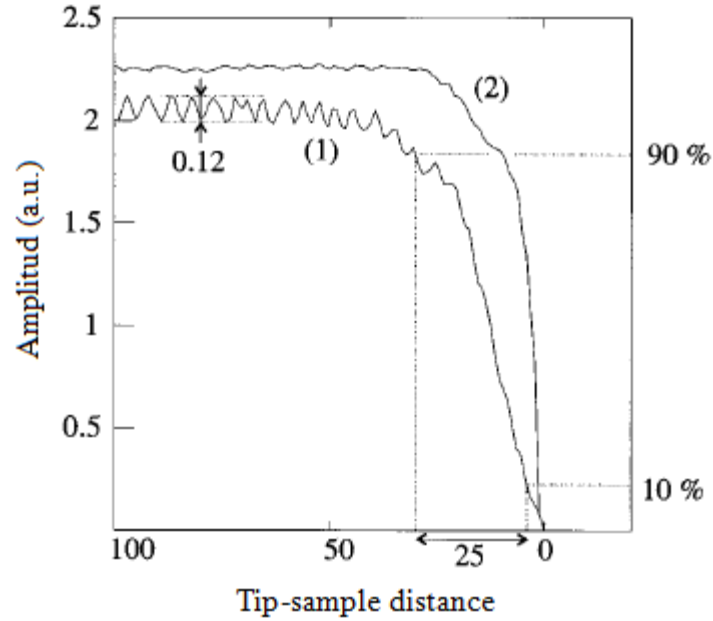


Figure 4. Approach curves: (1) detection through the tuning fork and (2) optical detection (arbitrary units)

The research done by Simon *et al.* [25] shows that the use of fiber overtone resonance modes up to 3 MHz for shear-force distance control has two advantages for near-field microscopy. They explain that the higher frequency allows a shorter feedback loop time delay, which in turn allows scanning speeds of $100 \mu\text{m/s}$ on a sample with a 150 nm height variation over a $1 \mu\text{m}$ distance. They made the experiments on a hard semiconductor device and on a soft polymer sample to demonstrate a factor of 5 improvements in scanning speed when the dither frequency is increased by a factor of 20. The other advantage is a reduction of the minimum lateral force required for height regulation, which is important for soft samples. Modeling the piezoelectric detection system as a harmonic oscillator indicates a factor of 33 increases in lateral force sensitivity when using the third overtone resonance of a typical fiber tip. The system used in the experiments is showed in Figure 4.

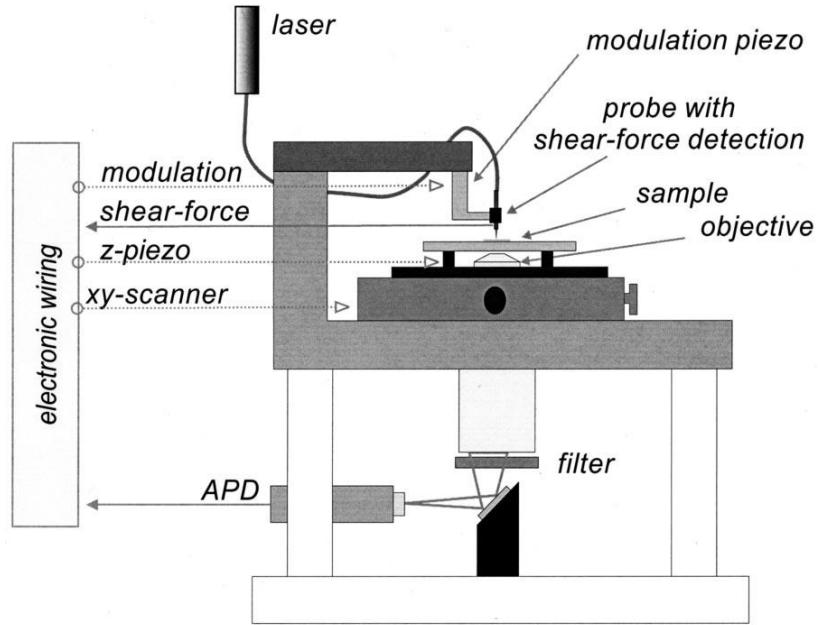


Figure 5. Near-Field optical scanning microscope head including fiber and shear-force tip-height detection apparatus [25].

As it is shown in Figure 5. The system has a similar structure to the system exposed in Figure 2. According to Simon *et al.* [25], a control loop such as their, consisting of an actuator, a sensor, and a feedback circuit, is characterized by the loop gain and bandwidth. The system becomes unstable if the loop gain is larger than 1, for frequencies where the phase shift is greater than 180° . They mention that maintaining a stable feedback loop puts an upper limit on the gain bandwidth product of the controller and thereby determines the maximum scanning speed.

Bruner *et al* [26], introduced an improved piezoelectric shear-force feedback system for tip-sample distance control in a scanning near-field optical microscope. They glued a tapered glass fiber into a metal tube and both were integrated in a mounting, sandwiched between two piezosegments. One of the piezoelements excites the fiber tip at mechanical resonance while the other one is used for detection. During the surface approach, the fiber resonance is damped by shear forces, which is registered by the second piezoelement and used for distance control. The main attraction in this setup is simplicity, compactness, and the lack of disturbing light sources. The fiber is

easy accessible and tip exchange is simple. With acceptable fiber amplitude of 5-10 nm (peak to peak) they obtained a topographical resolution of $5 \text{ pm}/\sqrt{\text{Hz}}$. This geometry allows the measurement of samples covered with a few millimeters of liquid, which is important for applications in biology and medicine.

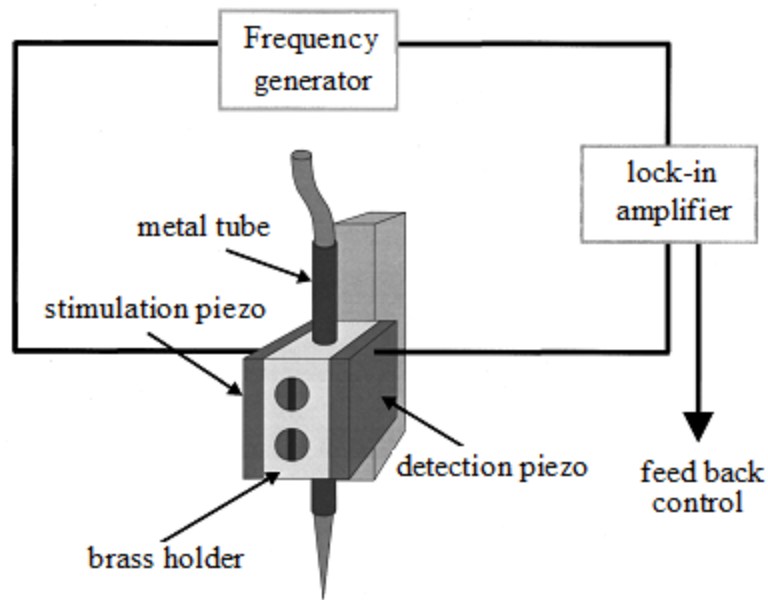


Figure 6. Illustration of the piezoelectric shear-force detection setup. [26]

Figure 6 describes the detection setup used by Bruner *et al.* [26]. The tapered glass fiber is glued into a metal tube and fixed with two set screws in a tiny brass holder, sandwiched between two piezoplates. The stimulation piezo excites the tip at its mechanical resonance. The response signal is registered by the detection piezo and measured with a lock-in amplifier. The change in amplitude and phase during the surface approach is used for distance control.

On the same research they say that the oscillation amplitude of the fiber tip is a very crucial parameter in near-field microscopy, so it is important to use very small fiber amplitude to preserve the optical resolution given by aperture. Another important topic is calibration; this was done in the experimentation by comparing the signals of the optical and the electrical shear-force setups as Salvi *et. al.* [25] did it.

Additionally Brunner *et al.* [27], describe a mode of shear-force feedback in which an additional vertical modulation is introduced. They refer to a modulated shear-force technique that deals with problem due to the snap to contact and therefore improves the mapping of soft and ductile materials, such as biological samples and soft polymers. Furthermore the modulated shear-force technique that they propose allows a simple comparison between effects in the optical far field an in the optical near field.

2.2. Quartz Tuning Fork

Quartz tuning forks (QTF) have been used in many applications as a means of sensing signal, particularly for acoustic and force microscopy [28,15], due to its physical feature consisting in a high mechanical quality factor Q , providing a very high sensitivity. The main advantage of using the quartz tuning forks, as a means of sensing shear forces, is that provides an electrical signal proportional to the shear forces that attenuate the vibration of the probe making them simple to operate, implement and control compared to optical force measurements techniques. Moreover, knowing the characteristics of resonance tuning fork, it is possible to make it vibrate at one of its resonance frequencies previously tuned, in order to get a high sensitivity, through a mechanical coupling with the probe, QTF can transmit the mechanical vibration necessary to use the shear force technique. The strategy is to characterize the frequency response of tuning fork vibrating to find the frequency of resonance observing the induced current. Figure 2 (a) shows a tuning fork package, which is used as a frequency generator to synchronize electronic systems, (b) it is a tuning fork without covering.

QTF can be designed to resonate at any frequency between 10 and 150 KHz range and beyond, in this experiment a 32.768 KHz QTF is used. Mechanical and electrical properties were extensively studied by Karrai and Grober [15]. Typically, the quartz tuning fork has a resonant frequency determined by its physical characteristics, as well as the mechanical properties of quartz, and is determined as follows:

$$f_o = \frac{\sqrt{WT}}{L^2} \sqrt{\frac{E}{p}}, \quad (1)$$

where W is the thickness, width, and T the length of the arms of QTF, E and p the Young's modulus and density of quartz respectively, whose values are $E=7.87E-10$ y $p=2650$ kg/m³. In this way, it is easy to verify that resonance frequency of a standard QTF ($L=3.12$ mm, $W=0.352$ mm, $T=0.402$ mm) is approximately 32.768 KHz, this value varies slightly because of manufacturing imperfections. Quartz is piezoelectric material

that can be simulated as a RLC behavior as it is showed in Figure 7. The input and output of circuit represents the QTF pins.

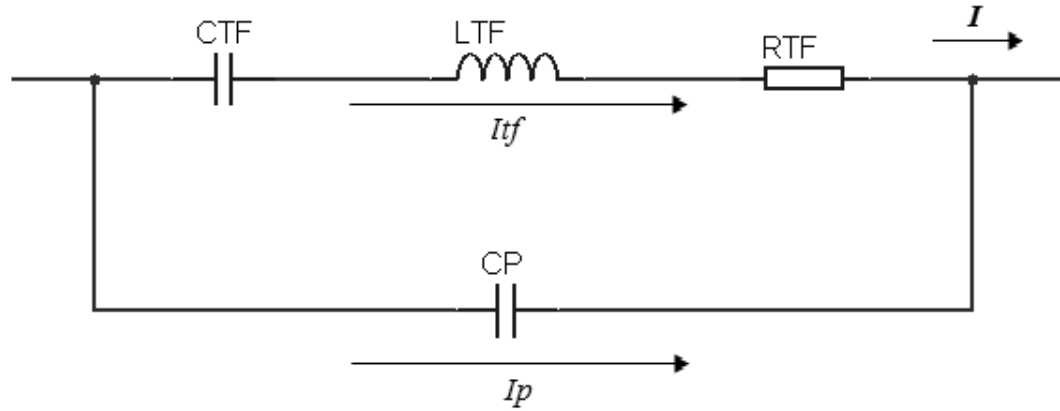


Figure 7. Equivalent circuit of a quartz tuning fork. CTF, LTF, RTF, and I are the capacitance, inductance, resistance and current, respectively, characteristic of QTF. Cp and Ip are the capacitance and current parasitic. Finally I is the current generated by the system.

As it was established before, the quartz tuning fork can be simulated like an electronic circuit with capacitance and current parasitic, this is because the capacitive contribution interferes to piezoelectric current; in order to eliminate the effect of the parallel stray capacitance, it was used the circuit shown in Figure 8, which is based on the electronic circuit proposed by Karrai [22].

The voltage V_{in} in Figure. 8 is a V_{ac} with a frequency defined by a signal generator; varying the frequency in generator, it is possible identify the behavior of tuning fork at certain values, in order to obtain the resonance frequency of tuning fork that it is around 32.768KHz according to the fork type. The resulting current is measured as a voltage V_{out} dropped across R, the load resistor. The response of circuit is shown in Figure 9. Before experimentation, it is necessary to remove the tuning cover, after that the fiber can be added to the tuning fork and experimentation can be done.

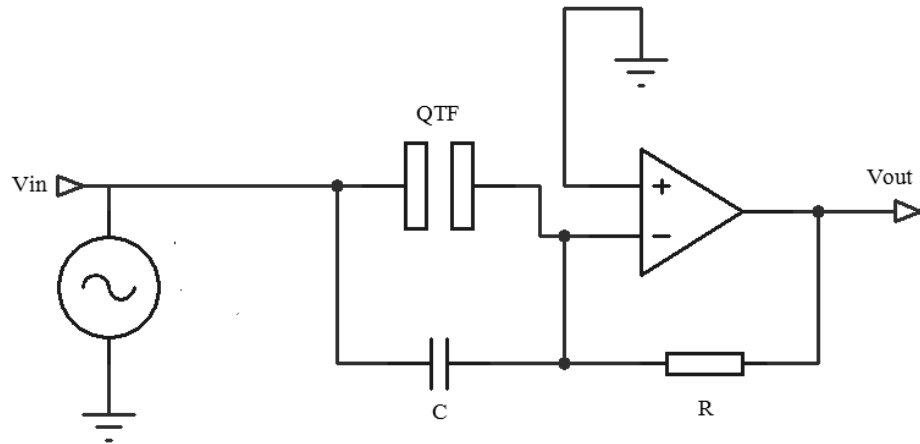


Figure 8. The tuning fork is driven by a voltage source V_{in} through a signal generator, where the QTF is the equivalent circuit of the tuning fork in Figure 7, C and R are the capacitor and resistor of the bridge circuit that allows eliminate the capacitance parasitic of tuning fork.

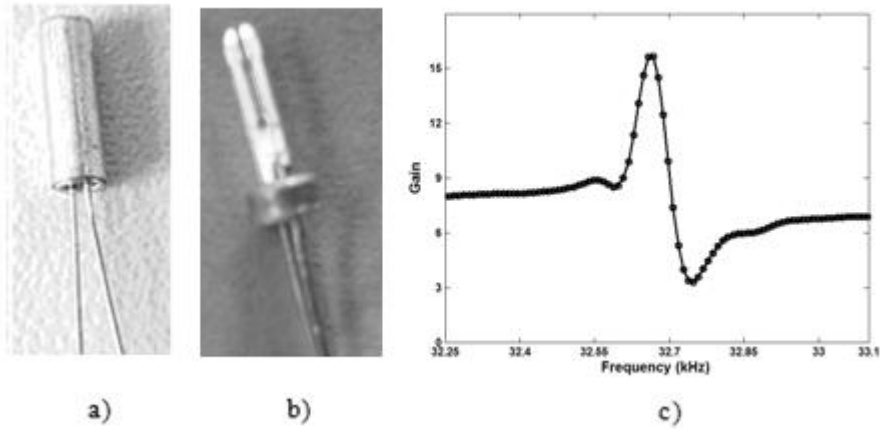


Figure 9. Tuning fork encapsulated (a) and cover removed (b) and finally its resonance curve obtained from experimentation (c).

2.3. Fuzzy Control Strategy Design

Fuzzy Logic is a paradigm for approximating a functional zapping [29]. In the last years the Fuzzy Control has increased his popularity, especially for algorithms used in the electronic, computing fields and others; such is the case of what occurs with some digital cameras that handle complex algorithms to take photos in spite of the movement, or in the case of the computing, with algorithms of web research. It is a strategy of control that has showed to be a powerful tool, especially because it allows controlling multi-variable processes with relative ease. The application of fuzzy set theory [30] is used to control robots and nonlinear processes. Due to the nonlinear behavior of piezoelectric bimorph used in the configuration, this control strategy is proposed in this work to implement in the control distance by shear force.

Fuzzy logic was developed by Lotfi A. Zadeh [30], on which the fuzzy control is based. This logic is inspired by the human thinking and natural language; it is basically an effective means for obtaining real-world data and processes it in a system of inferences. Practically it allows a relationship between number processing and natural world based on human reasoning. For example stature can be classified as high, very high, low etc. and based on this classification it is possible to process information using fuzzy logic assigning membership values to each one. Unlike traditional Boolean logic, this type of strategy covers the whole spectrum and not only absolute options (0 and 1, all or nothing) on the basis of a language such as referring to a color as medium dark, very blue or a little gray; from this terminology, it applies nondeterministic mathematical models to generate a solution to control a particular process. In other words, through non-specific entries, a manipulation is obtained to control a system that could be multivariable or nonlinear as in the case of this work. One of the most important aspects of this control strategy are the membership functions, which can locate a variable in a certain range, then, after a series of rules that depend on the experience about the process and the inference designed, manipulation is determined to be proportional to the system in order to obtain the desired variable process value. Fuzzy control provides a formal methodology for representing a human's heuristic knowledge about how to control a process. Implementation of controllers based on

fuzzy logic is motivated for their ability to capture qualitative control strategies and their ability to implement a highly flexible control behavior.

The main concepts in fuzzy logic are Fuzzy sets, linguistic variables, Membership function, Fuzzy set theory, Fuzzy if-then rules. The above concepts will be described.

Fuzzy sets. A fuzzy set can be defined as a class of objects with continuous degrees membership. As the boundaries of a fuzzy set are not defined, it is not possible to determine the exact amount of component parts. To determine how much belongs to a group, the values of belonging or membership that define the elements vary between 0 and 1, where those who have membership values close to 0 means that it is unlikely that belongs to the set, and have membership values close to 1 means likely to belong to the set. The membership function of a fuzzy set A is denoted as μ_A . A fuzzy set A in U is expressed as a set of ordered pairs:

$$A = \{(x, \mu_A(x)) | x \in U\}. \quad (2)$$

Linguistic variables. A linguistic variable is a variable whose values are words or sentences in a natural or artificial language. The words are characterized by fuzzy sets defined in the universe in which the variable is defined. Linguistic variables are used to convert numerical values into qualitative ones; a numerical variable takes numerical values: height=180 m; a linguistic variable takes linguistic values: height = tall. The linguistic values of a linguistic variable can be described as follows [34]:

- 1.- qualitatively using an expression involving linguistic terms (adjective) and
- 2.- qualitatively using a corresponding membership function.

Membership functions. In order to define what is the value of membership of an element with respect to a point using the membership functions, which mathematically define the value of each item by using mathematical equations, there are several types of membership functions, the most commonly used are:

Triangular membership function. Triangular membership function is defined by 3 parameters a , b and c , where $a < b < c$ are the points of each of the corners, the equations that define the triangular membership function are shown in Equation 3. and Figure 10.

$$\text{trimf}(x; a, b, c) = \begin{cases} 0, & x < a \\ \frac{x-a}{b-a}, & a \leq x \leq b \\ \frac{c-x}{c-b}, & b \leq x \leq c \\ 0, & x > c \end{cases}. \quad (3)$$

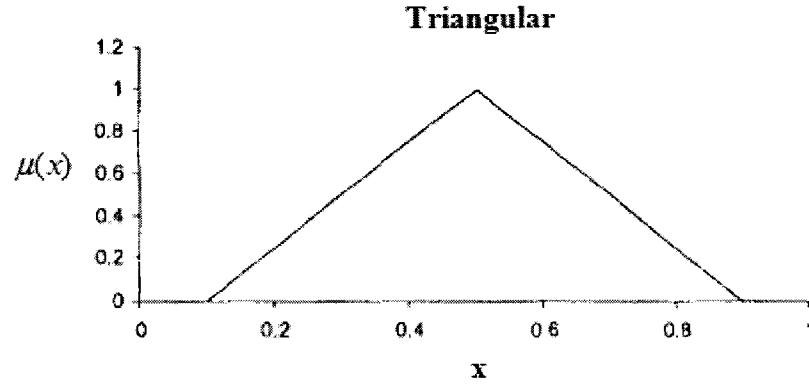


Figure 10. Triangular membership function

Trapezoidal membership function. Unlike the triangular, this requires additional parameter d , $a < b < c < d$ as well as the triangular function points indicate the corner. Trapezoidal function is shown in Equation. 4 and Figure 11.

$$\text{trapmf}(x; a, b, c, d) = \begin{cases} 0, & x < a \\ \frac{x-a}{b-a}, & a \leq x \leq b \\ 1, & b \leq x \leq c \\ \frac{d-x}{d-c}, & c \leq x \leq d \\ 0, & d < x \end{cases}. \quad (4)$$

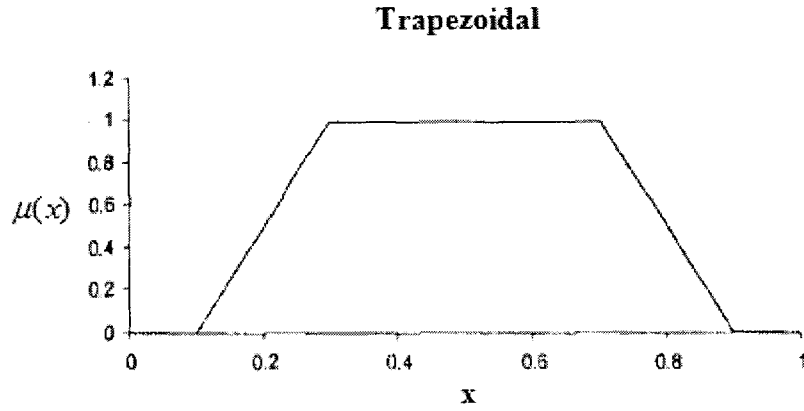


Fig. 11 Trapezoidal membership function

Gaussian membership function. This function is defined by parameters m and σ representing the center and width of the function respectively, it differs from the above figures because it can be defined by a single equation that covers the entire range of the membership function as it is shown in Equation 5 and Figure 12.

$$gaussmf(x; m, \sigma) = \exp\left(-\left(\frac{x-m}{\sigma}\right)^2\right). \quad (5)$$

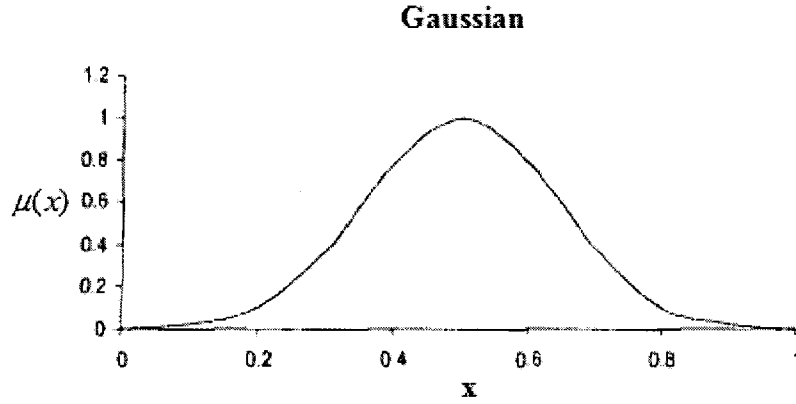


Fig. 12. Gaussian membership function

Bell Membership Function. It is defined by the parameters a , b , c , where b is usually positive for the bell pointing upwards and defines how the hood, for small values, the bell tends to be pointed, and for large values, the bell tends to be square, to define the width of the bell c defines the center. This function differs somewhat from the Gaussian and its width also varies and is defined as shown in Equation 6 and Figure 13.

$$bellmf(x; a, b, c) = \frac{1}{1 + \left|\frac{x-c}{a}\right|^{2b}}. \quad (6)$$

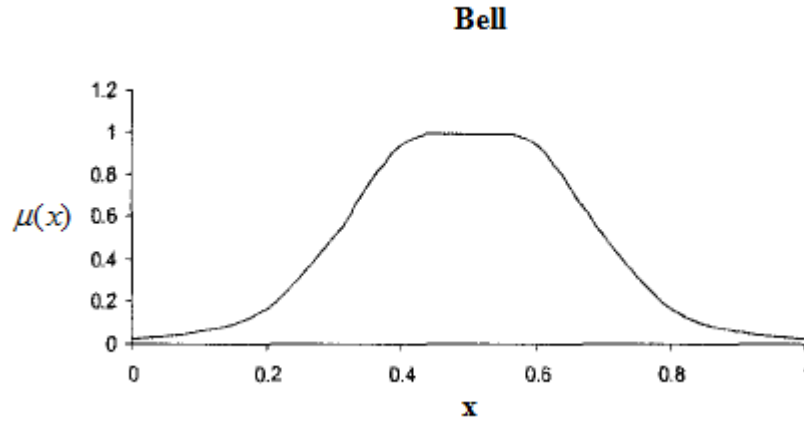


Figure 13. Bell membership function

Fuzzy set theory. Fuzzy set theory generalizes the conventional set theory [30]. Then, the axiomatic foundation becomes different from the classical set theory. Particularly, two basic laws of Boolean algebra differ with Fuzzy set theory, the law of excluded middle $A \cup \bar{A} = U$ and the law of contradiction $A \cap \bar{A} = \phi$.

In general, fuzzy control consists in four main sections [29]: The rule base section has the knowledge arranged in a set of rules about how to control the system. The inference machine classifies which control rules established on rule base section are important and relevant, then in function of the rules that are activated, decides the control action to perform at current. Fuzzification element modifies and transforms the input variable in control system so that it can be compared and interpreted by the inference machine according to the rules defined. Defuzzification block converts the conclusions reached by the inference machine into the input range to the plant. Figure 14 shows the fuzzy controller scheme.

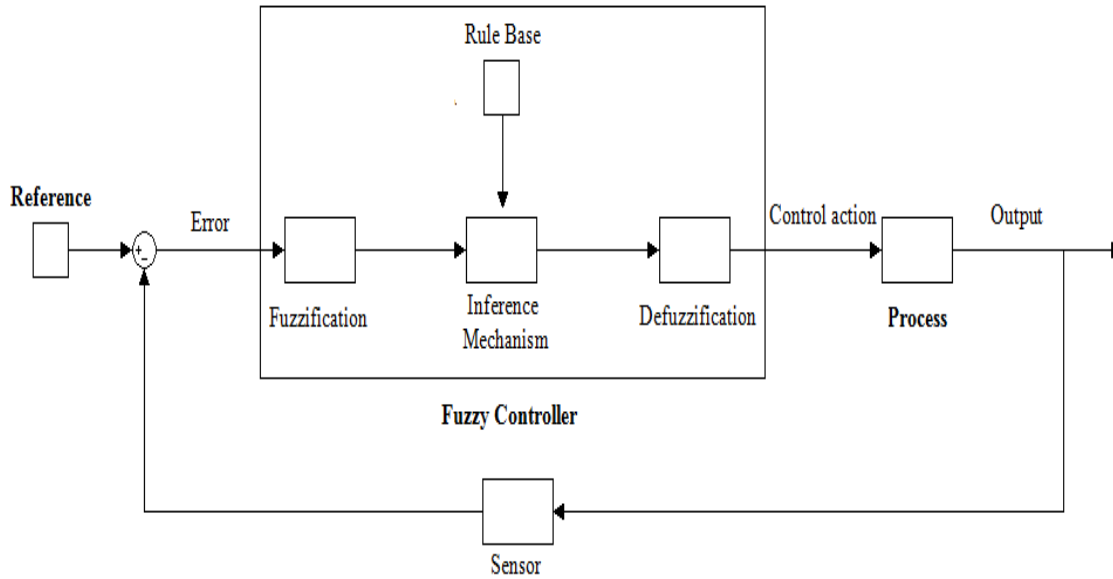


Figure 14. Fuzzy controller scheme

The fuzzy controller can be viewed as an artificial decision maker that is able to send control responses in real time. Basically, it compares the reference input with the plant output data and according to the rule base on the inference machine decides and sends the necessary manipulation of the plant to maintain the stable reference point. The empirical knowledge, many times this experience comes from human operators who process the plant and understand the plant dynamics to control it under a series of human rules or perspectives.

Fuzzy if-then rules.

In the fuzzy design, these rules basically have the following structure: “If-Then”, where if has the condition and then the control response action. According to Passino [29], the general form of the linguistic rules is

$$\text{If premise Then consequent} \quad (7)$$

The premises or antecedents are linked with the fuzzy controller input and are located to the left side of the rules. The consequents or actions are associated with the fuzzy controller output and they are on the right side of the rules.

Otherwise, the inference engine takes place when the rules get on and it is necessary to process the results on rules. First, the premises of all rules are compared to the controller input to find which rules were applied at current process. Then, the conclusions or the control actions are determined by a fuzzy set that indicates the appropriate manipulation output in order to keep the error process around practically zero, in other words, the control action necessary to have the desired set point through a regulatory mechanism.

There are a number of relations that can represent the meaning of IF X is A then Y is B. The most used implications in fuzzy sets are:

Implication of Lukasiewicz: This implication is based on the equivalence $p \rightarrow q \equiv p \vee q$. To represent OR is also possible to use the limited sum $\min(1, 1-p+q)$ instead of the maximum $\max(p, q)$. This results in the relation called R_a , defined as

$$\mu_{R_a}(x, y) = \min(1, 1 - \mu_A(x) + \mu_B(y)). \quad (8)$$

Implication of Mamdani: This is the most important implication known in literature, with respect to fuzzy control. Its definition is based in the intersection. The relation R_c (x of conjunction) is defined as:

$$\mu_{R_c}(x, y) = \min(\mu_A(x), \mu_B(y)). \quad (9)$$

Implication of Zadeh: In logic of two values, $p \rightarrow q$ has the same true values as $p \wedge q \vee p$. This equivalence was used by Zadeh in the next form:

$$\mu_{R_m}(x, y) = \max(\min(\mu_A(x), \mu_B(y)), 1 - \mu_A(x)) \quad (10)$$

Inference engine. There are two basic types of approaches employed in the design of the inference engine of a fuzzy controller: composition based inference and individual rule based inference. The design parameters for the inference engine are as follows:

- Choice of representing the meaning of a single production rule,
- Choice of representing the meaning of the set rules,
- Choice of inference engine,
- Testing the set rules for consistency and completeness.

Fuzzification Module. The fuzzification module (FM), according to [31] performs the following functions:

- FM-F1: Performs a scale transformation (input normalization) which maps the physical values of the current process state variables into a normalized universe (normalized domain). It also maps the normalized value of the output variable onto its physical domain.
- FM-F2: Converts a point-wise (crisp), current value of process state variable into a fuzzy set, in order to make it compatible with the fuzzy set representation of the process state variable in the rule-antecedent.

Defuzzification. The functions of the defuzzification module (DM), according to [31], are as follows:

- DM-F1: Performs the so-called defuzzification which converts the set of modified control output values into a single point-wise value.
- DM-F2: Performs an output denormalization which maps the point-wise value of the control output onto its physical domain.

Two of the most used defuzzifications operators are Center of Area and Mean of Maximum.

Center of Area: The method of center of area or gravity center is the most known defuzzification method. For a discrete case, it is defined as:

$$y^* = \frac{\sum_{i=1}^l y_i \cdot \mu_Y(y_i)}{\sum_{i=1}^l \mu_Y(y_i)} = \frac{\sum_{i=1}^l y_i \cdot \max_k \mu_{CLY(k)}(y_i)}{\sum_{i=1}^l y_i \cdot \max_k \mu_{CLY(k)}(y_i)} \quad (11)$$

In the continue case, it is obtained as:

$$\mu^* = \frac{\int_y u \cdot \mu_Y(y) dy}{y \int_y u \cdot \mu_Y(y) dy} = \frac{\int_y y \cdot \max_k \mu_{CLY(k)}(y) dy}{\int_y \max_k \mu_{CLY(k)}(y) dy} \quad (12)$$

Mean of Maximum: This method determines the first and last values, where Y has a maximum degree of membership and then it takes the mean of those two values. Formally,

$$y^* = \frac{\{\inf y \in \gamma \mid \mu_Y(y) = hgt(Y)\} + \sup\{\inf y \in \gamma \mid \mu_Y(y) = hgt(Y)\}}{2} \quad (13)$$

3 EXPERIMENTATION

3.1. Schematic System

The schematic diagram of the system consists basically in a reference signal input by a signal generator. This sinusoidal reference signal is sent to the tuning fork to produce mechanical vibrations caused through a mechanical coupling with the fiber, which permits sensing shear forces of sample. Furthermore, the sinusoidal reference signal is previously conditioned by the data acquisition card (DAQ), in the same way, DAQ receives the tuning fork sensing signal, thus comparison is made and then it sends signals to the error signal software to block fuzzy controller, there was weighted the error and sends a signal handling high voltage system, which amplifies it and sends it to the piezoelectric bimorph, the actuator exerts finally mechanically control the action, seeking compensate the error obtained by the tuning fork. Figure 15 describes the schematic system.

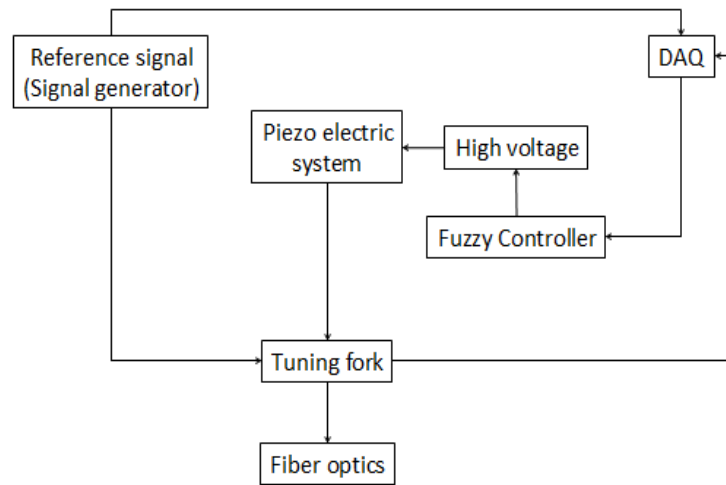


Figure 15. Schematic of shear force control system.

In the previous schematic figure, the piezoelectric system is the actuator that allows running physically the control action sent from controller block. In Figure 16, it is possible to observe the real piezoelectric used in the practical experimentation, this piezoelectric device has three piezoelectric bimorphs which have a hysteretic phenomena characterized by Ando *et al.* [32]. Basically, piezoelectric bimorphs consist

of two flat strip of piezoelectric elements joined one to each other, provided with electrodes in such a way that when an electric field is applied, one strip elongates while the other contracts [33], this characteristic is useful to manipulate the distance between fiber and sample. Each piezoelectric represents an axis in the space such it is possible to scan moving x and y axis and controlling z distance; in the middle of the three axis there is a tube welded which contains the fiber probe; also there is a triangular prism to obtain the reflect probe tip and calibrate the system.

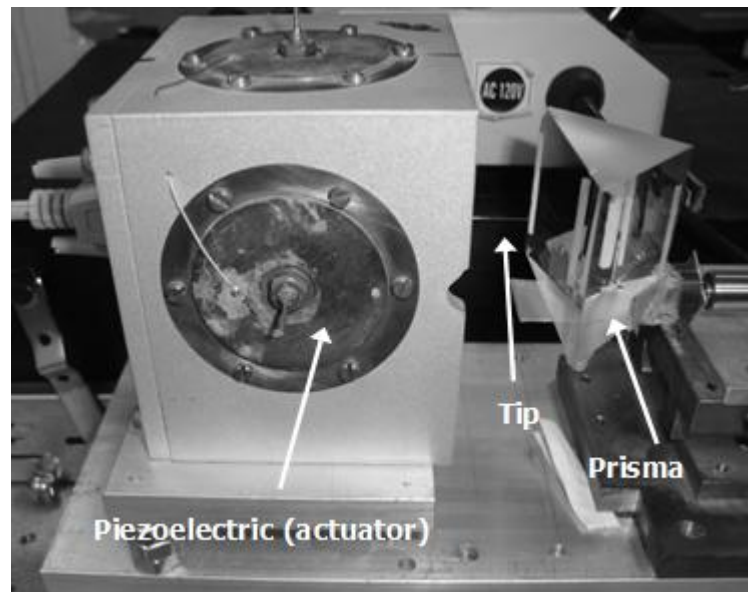


Figure 16. Piezoelectric and probe set up.

The high voltage block in Fig. 15 has two main components: high voltage amplifier and high voltage source, the first one needs the second one because the operational amplifier used (PA88) needs up to 100 volts at direct current to operate the bimorph piezoelectric in the operational zone. Fig. 17 shows the high voltage source circuit implemented to feed the operational amplifier. It has basically two stages: rectification and filtering. Rectification is realized by four electrodes that convert alternating current to direct current. Filter stage consist in an resistor-capacitor arrangement to eliminate the slight ondulation from rectification stage. The vdc at output is around 170 volts; enough to operate the operational amplifier PA88.

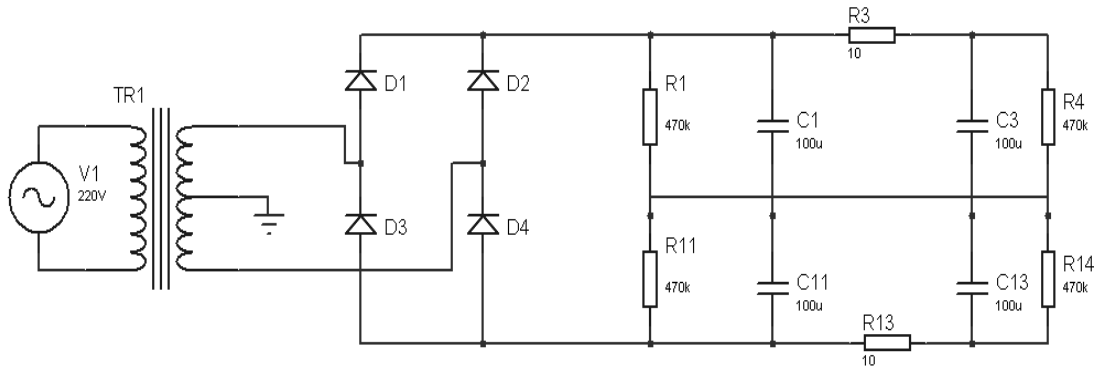


Figure 17. High voltage source circuit to operate the operational amplifier PA88.

The DAQ output level is in a range of 0-4 volts dc so then, with a gain of 40 in the operational amplifier electronic configuration, it is possible to obtain a high voltage range between 0 and 160 volts to excite the piezoelectric bimorph and manipulate the vibration on probe. Figure 18 describes the electronic configuration used to amplify the signal sent by controller with the objective to feed the piezoelectric and compensate in a mechanical manner the distance between tip and surface.

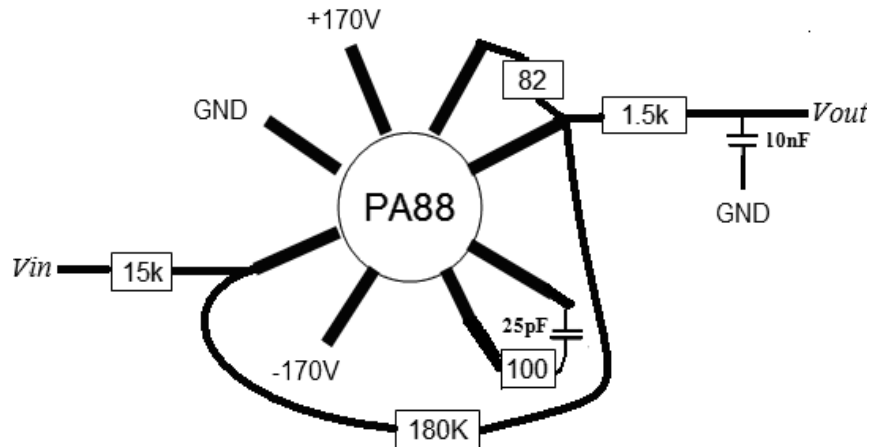


Figure 18. Operational amplifier PA88 electronic configuration.

3.2. Calibration

The system needs to be configured and calibrated; therefore it is necessary to find the resonant frequency of the QTF. As illustrated in Figure 19, the response of tuning fork has a maximum and minimum when a voltage ac is applied to the input of the circuit of Figure 8. If the signal frequency changes, the gain changes as well, prior to tune the resonant frequency of the tuning and identify the area of operation where the system is more sensitive. In the case of the QTF without the fiber this resonance must be around 32.768 KHz, as shown in Figure 19.

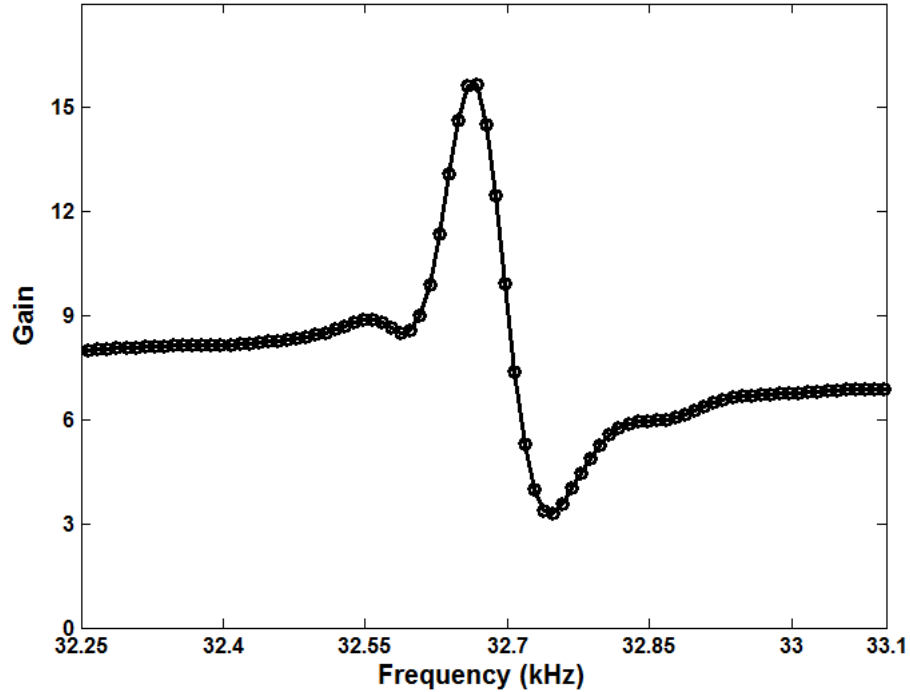


Figure 19. Frequency response of the tuning fork used without fiber.

Once you have identified the resonance frequency, the fiber is attached to one arm of the tuning fork at right angles. Subsequently, again using the circuit of Figure 3 to tune the resonant frequency of the system. It is expected that due to the weight of the fiber, the frequency response suffers any change or modification. Figure 20 shows how the tuning of the oscillation amplitude decreases strongly due to increased mass of the arm; in addition the fall of the resonance amplitude is weaker compared to fiber-free tuning of Figure 19. Additionally the resonance frequency decreases about 32.45 KHz as can be seen it in Figure 20.

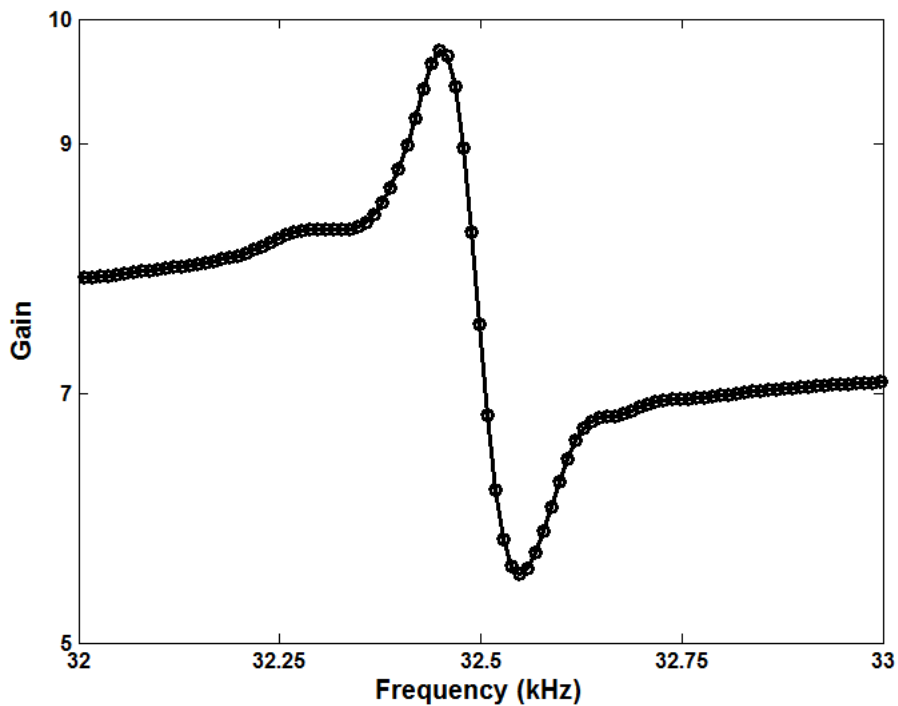


Figure 20. Frequency response of the tuning fork used with fiber

On the other hand, Figure 21 allows the comparison of the frequency response of a tuning fork with probe and without probe, previously listed, which shows that the amplitude and resonance frequency of the tuning fork is amended by adding the probe.

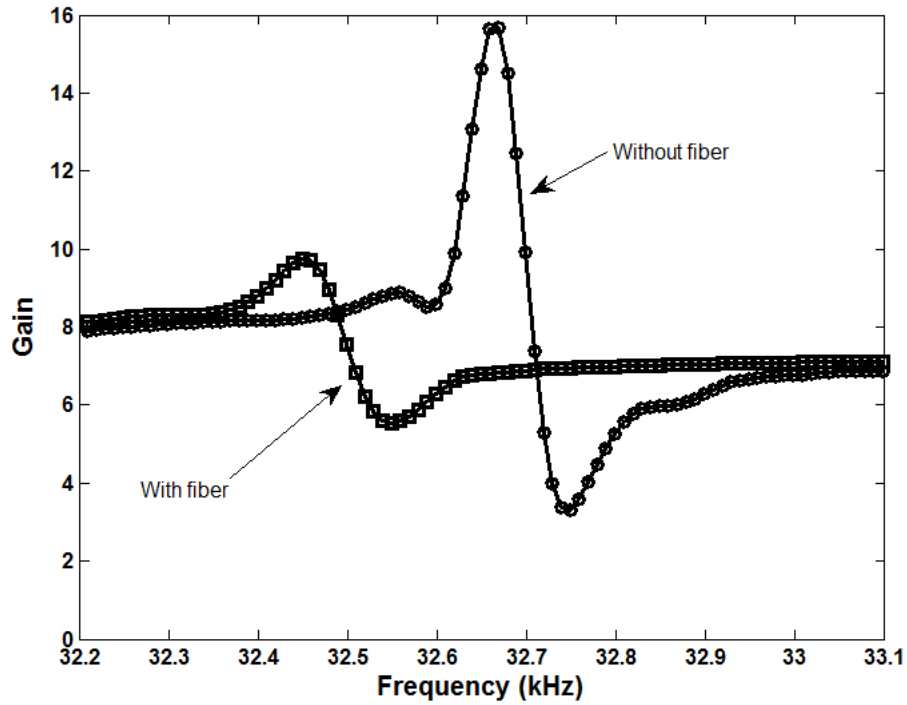


Figure 21. Frequency response comparison of the tuning fork.

Subsequently, after tuning the resonant frequency of the tuning fork with probe, it is necessary to identify the operation range of the system composed by the fiber coupled to the piezoelectric actuator and the sample surface. Tuning fork with fiber is placed on a tube welded to the piezoelectric bimorph functions as the axis z to control the tip-surface gap. Then, a prism is attached to a base with the objective of reflect the tip and bring the chance to observe the tip approaching, after that, using a resort system a first approximation is done and finally, using an external piezoelectric, a fine adjustment is performed, this occurs due to the input voltage applied to the piezoelectric bimorph. Figure 22 represents the physical set up of tuning fork and prism; using the resonant frequency found in Figure 20, when the tip is close enough to the prism surface to damp the vibration signal, the operation range zone takes place until the gap between tip and sample surface is zero, and the slop change is reduced to practically zero, therefore, the controller manipulation can be control the distance in that range.



Figure 22. Probe and prism set up.

This interaction between the probe and the sample is mainly governed by shear forces, which cause damping in the oscillation amplitude of the probe in a range that goes from 0 to 20 volts, where 20 volts represents the position $z = 0\text{nm}$. Due to the limitations of experimentation is not possible to establish with certainty the position of piezoelectric when it has an input voltage equal to zero and at the same time is situated at the beginning of the sensitivity range of the tuning fork. Figure 23 represents the shear forces interaction, which cause the attenuation in output system signal.

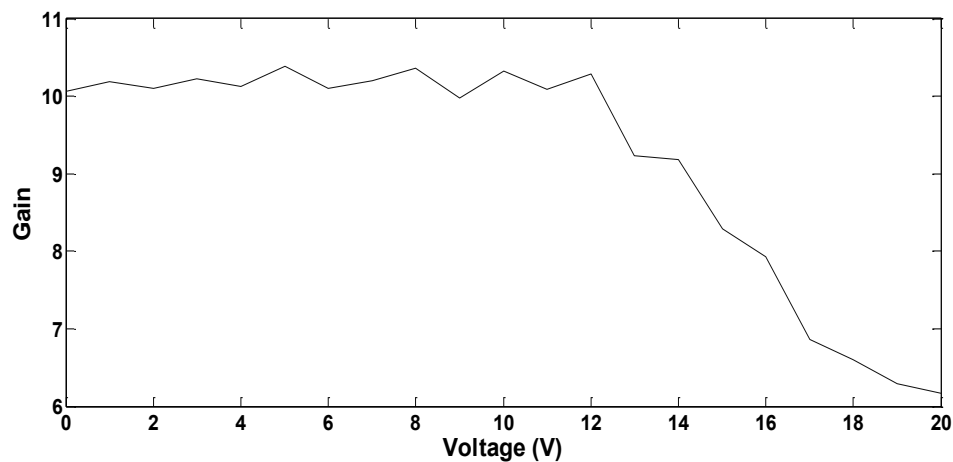


Figure 23. Attenuation of amplitude oscillation in the proximity of a surface clean and flat glass

3.3. Control Panel

The Human-Machine Interface (HMI) is configured on Labview software by National Instrument (8.2). The panel has two pages, in the Page 1 are the commands that allow to configured the system manipulation and control; there, the control mode can be chosen between manual and automatic control mode; manual control mode permits to modify the output manipulation OP according to user needs or configuration. OP has a range located between 0 and 5 volts, but for safety reasons, the data acquisition system (DAQ) is set to send 4 volts as maximum and 0 volts as minimum; also it is possible to see the current process value (PV), set point (SP) and output (OP), finally the panel has an emergency stop, see Fig.24; additionally, the control panel has two waveform chart, at top left there is the chart including the process value PV (rms) and the reference SP (rms); at bottom left is the chart showing the output manipulation OP, and error. Error variable is the current difference between the SP and PV. Finally, there are two control modes: Fuzzy control and Proportional-Integral-Derivative control (PID), the last has a Proportional-Integral function through K_c and T_i parameters.

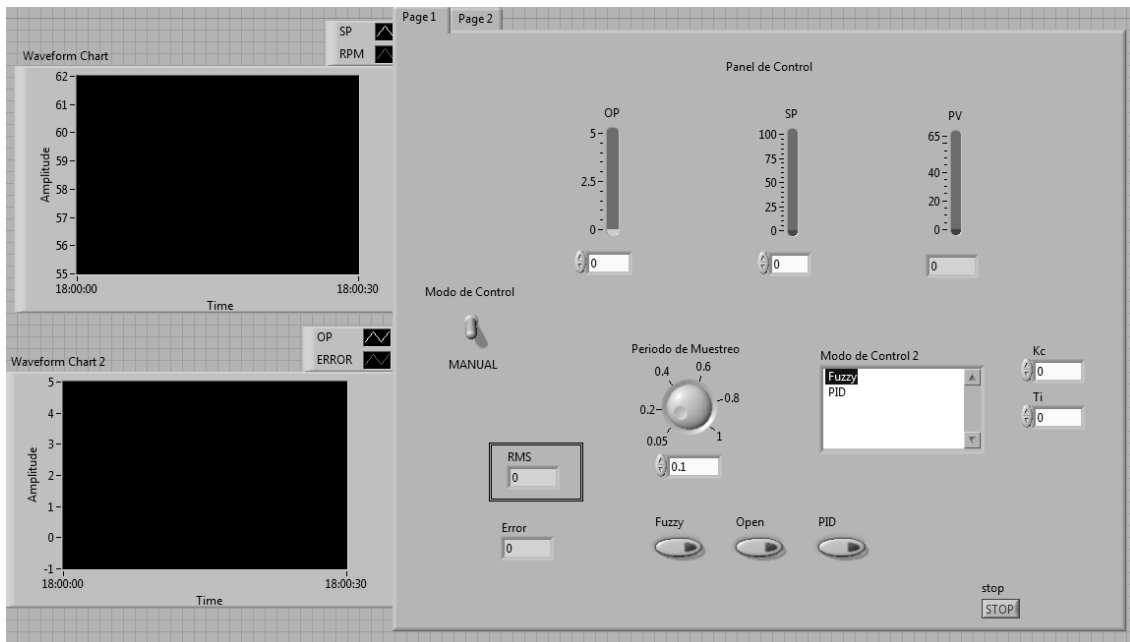


Figure 24. Control panel interface created using Labview software by National Instrument

On the other hand, there is a second page (Page 2) in the control panel. There is the control design, the membership functions of fuzzy controller; it is possible to observe that the three membership function chars (error, error derivate and output) are defined by crossing points designed by user, through these crossing points the membership functions are being established, in the particular case of the error and error derivate variables is done by triangular functions. The output variable has singleton as membership function as it can be appreciated on Figure 25.

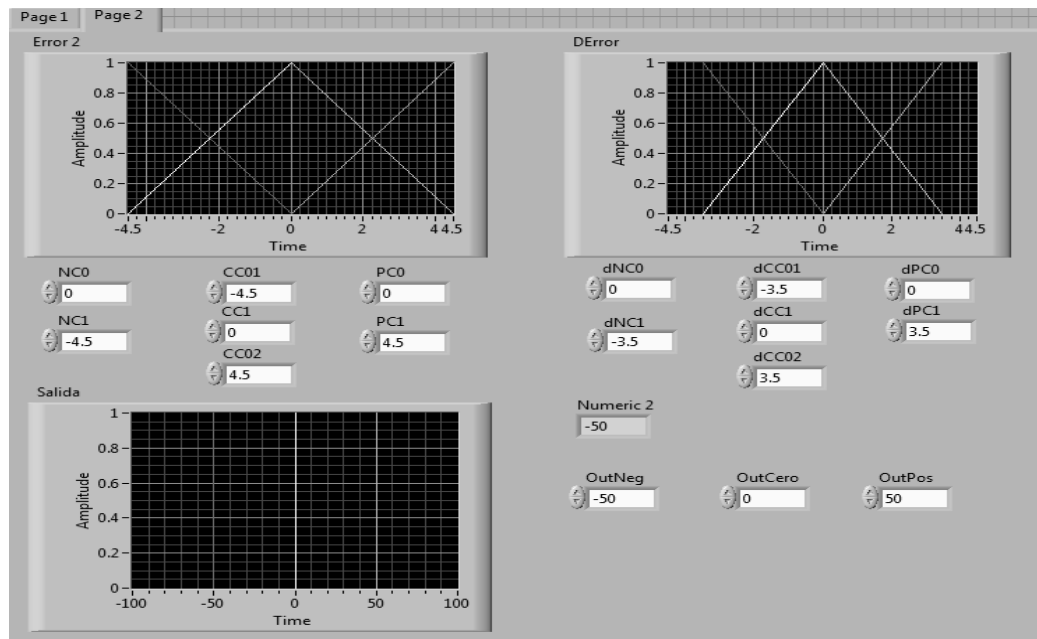


Figure 25. Fuzzy Control Panel

3.4. Fuzzy Control Strategy Design

The control system is established by the modules shown in Figure 26. A reference sinusoidal signal provides the desired set point of the system, the subtraction of the process variable and the reference desired signal must be close to zero, so the error is minimal. This is achieved by fuzzy controller, which receives the error signal, and according to the controller design, we established the membership degrees given by the previously defined membership functions. Subsequently inferences take place and fuzzification process sends a signal to the system manipulation. The controller output signal passes through a conditioning block; due to the characteristics of piezoelectric bimorph used, it is necessary to have high voltages in the range of 0 to 140 volts in order to produce the displaced required in the actuator, then, it is necessary to amplify the output signal from the controller. After amplifying, the manipulation signal is supplied to the piezoelectric. Finally, the electronic arrangement allows tuning fork sensing vibration changes caused by shear forces in sampled surface; the measured signal is conditioned to be compared again with the reference signal.

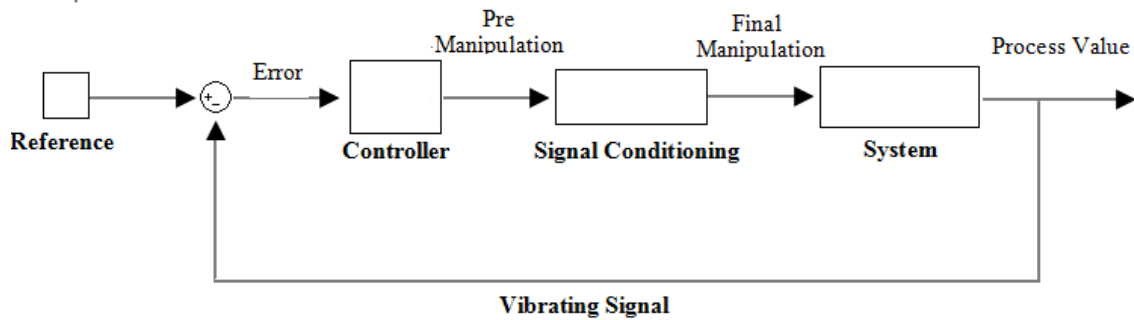


Figure 26. Control block diagram

According to the control design, It was established two input variables and an output variable; input variables were called error and derror where error refers to the difference between the desired value and the process value and derror correspond to the error tendency; error membership functions has a domain from -5 to 5 volts, derror from -4 to 4 volts, and output membership is configured using singleton functions, so

the domain is -1.5, 0 and 1.5 volts. Singleton was because it brings the advantage to process information in a reliable and practical form, mainly at defuzzification process. Membership functions were chosen and designed according to the operation range found it in experimentation; in this case the tuning fork has an operation range between 6 and 9 rms volts a.u. and the output manipulation is conditioned to operate in a 0-4 volts range. The membership functions were normalized with respect 5 volts. Figures 27, 28 and 29 shows the membership functions used in this work.

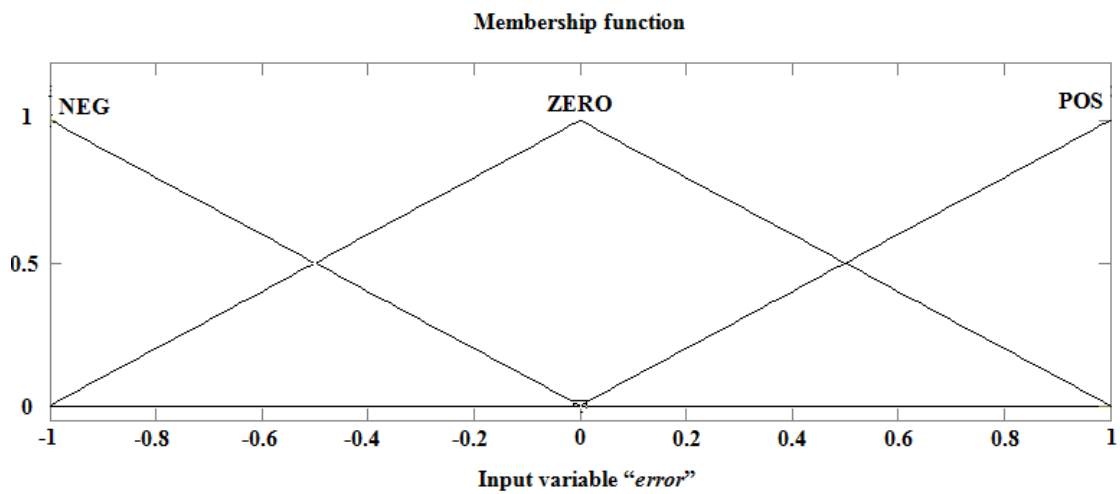


Figure 27. Normalized error membership function.

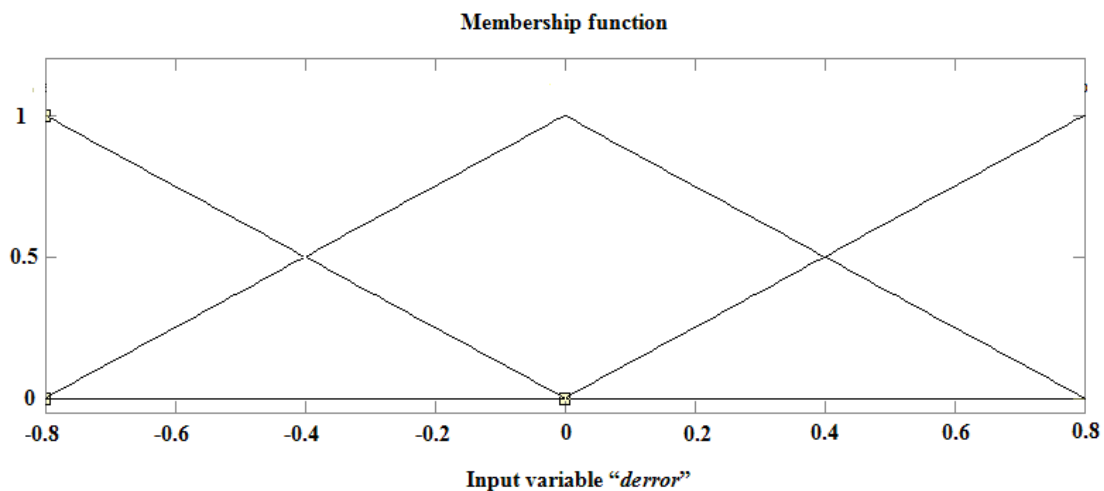


Figure 28. Normalized error derivate membership function.

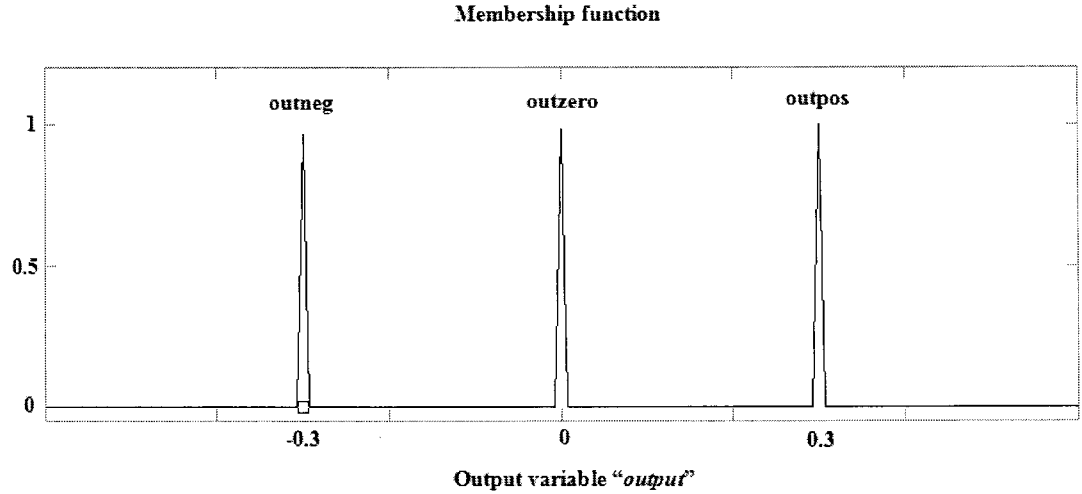


Figure 29. Normalized output membership function.

The error equation is given by the following equation

$$er = yd - y \quad (14)$$

where er is the error system, yd is the set point or the desired value and y the current process value, so that when the error is positive then the process variable is below the desired value, and when the error is negative means that the process variable has exceeded the set point. Now, the error derivate (derror) is given by this equation:

$$de = er - ea \quad (15)$$

where er is the current error and ea is the previous error. Below in Fig. 30 the inference rules established in the controller design are shown, and Fig. 31 describes the control surface of the fuzzy stabilization rule base for the distance control.

1. If (ERROR is NEG) and (DERROR is neg) then (OUTPUT is OUTPOS) (1)
2. If (ERROR is ZERO) and (DERROR is neg) then (OUTPUT is OUTZERO) (1)
3. If (ERROR is POS) and (DERROR is neg) then (OUTPUT is OUTNEG) (1)
4. If (ERROR is NEG) and (DERROR is zero) then (OUTPUT is OUTPOS) (1)
5. If (ERROR is ZERO) and (DERROR is zero) then (OUTPUT is OUTZERO) (1)
6. If (ERROR is POS) and (DERROR is zero) then (OUTPUT is OUTNEG) (1)
7. If (ERROR is NEG) and (DERROR is pos) then (OUTPUT is OUTPOS) (1)
8. If (ERROR is ZERO) and (DERROR is pos) then (OUTPUT is OUTZERO) (1)
9. If (ERROR is POS) and (DERROR is pos) then (OUTPUT is OUTNEG) (1)

Figure 30. Fuzzy rule base for distance control by shear force technique

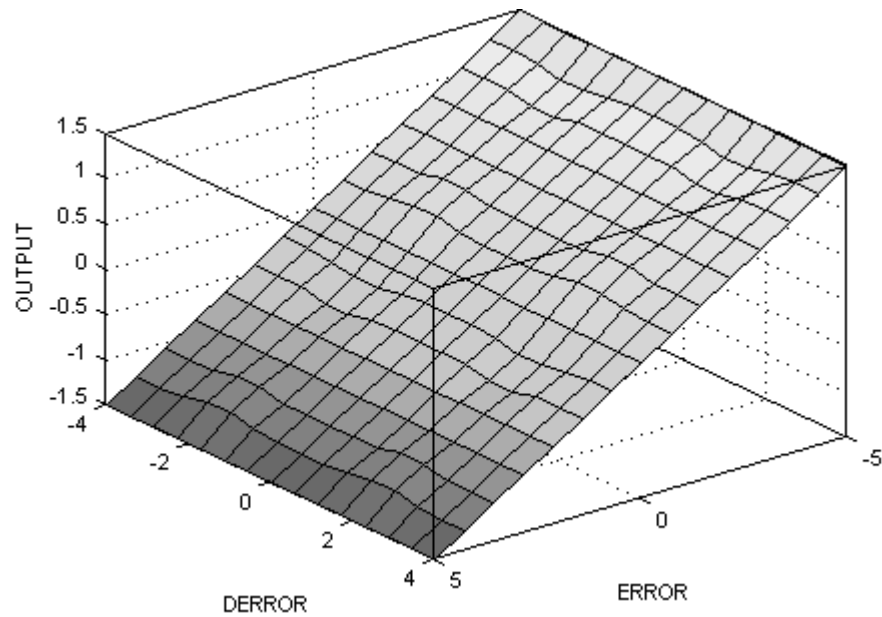


Figure 31. Surface of the fuzzy stabilization rule base

The system trajectory of the fuzzy design is mapped on the partition space in Figure 32. The illustration shows a tendency to cover the error domain. Nevertheless, it has stabilization on the zero zones.

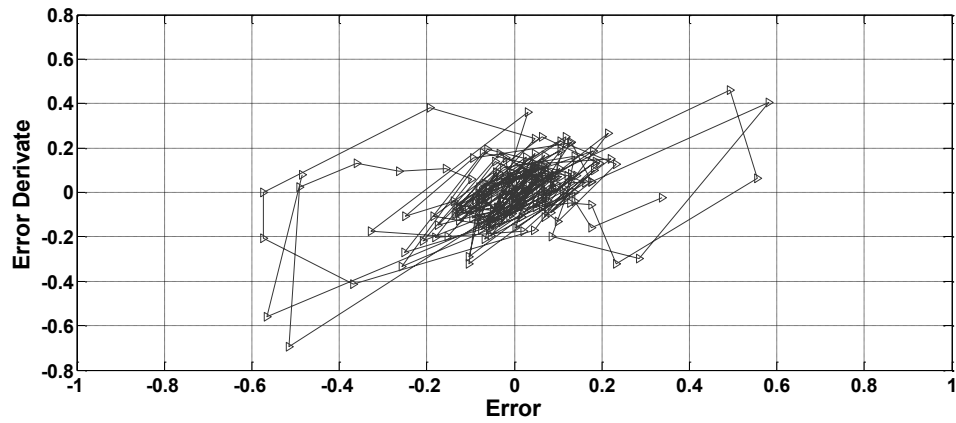


Figure 32. System trajectory of the fuzzy design mapped.

3.5. Experimental Results

In order to view the control action system, it has been used external piezoelectric, which, by supplying a type excitation step, a movement that simulates a surface relief, this experimental technique was proposed by Grober *et. al.* [20]. The pulse is the system perturbation (discontinuous line) and the control response (continuous line) represents the compensation by the controller. It is important to mention that the control designed in this work is focused on the regulation system; the main objective is to maintain a constant distance between the sample surface and probe and to have a control response as much as possible proportional to the perturbation in the system.

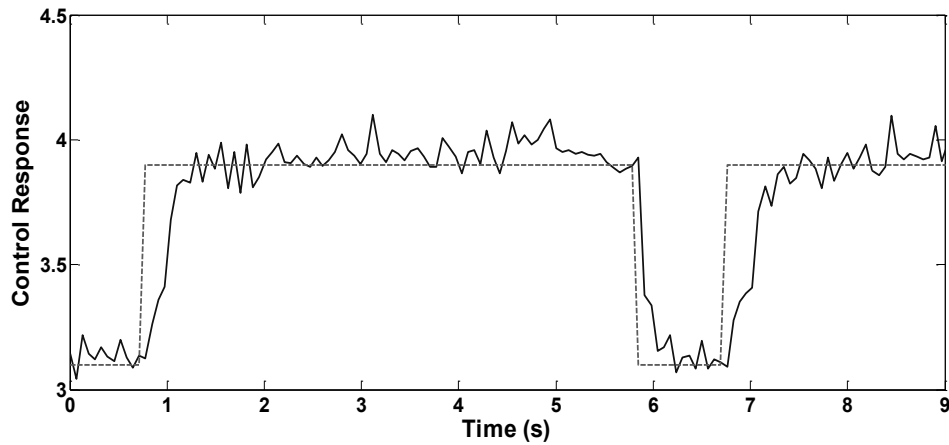


Figure 33. Fuzzy control response.

In Figure 33, the fuzzy control response from the controller proposed has a control effort which oscillates around 0.2 a.u. and it tends to stabilize near of the discontinuous line (3.9 a.u. and 3.1 a.u) which represents the perturbation in the system. Figure 34 shows the dispersion in the control response.

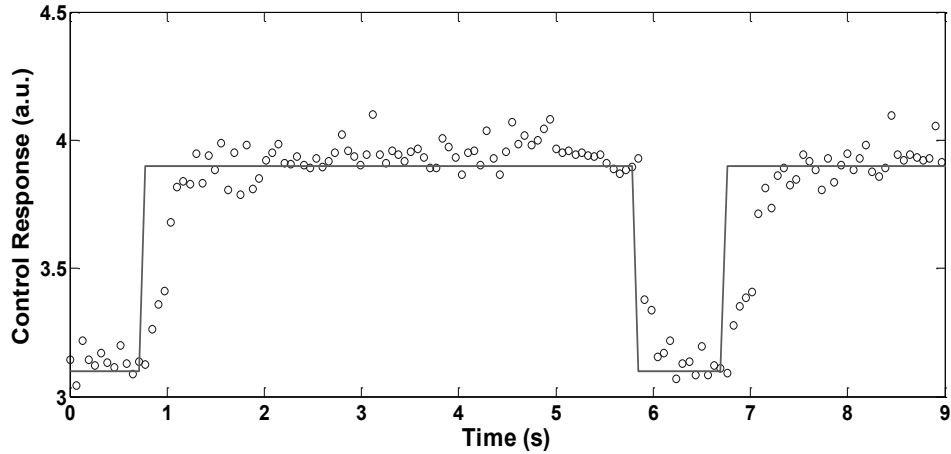


Figure 34. Dispersion of the fuzzy control response.

It was mentioned before that Grober *et. al.* [20] designed a similar experimentation to simulate a sample surface. They used a proportional and integral controller in order to keep the distance between the probe and the piezoelectric. Nevertheless they obtained a control effort with oscillatory trend to compensate perturbations. It results important to analyze the control response for a proportional integral controller (PI), trying to have similar conditions that the fuzzy control experimentation. It was necessary to tuning the PI controller; this was obtained by an open loop experimental set up and trial and error method, because the actuator has a non-linearity that modifies the PI parameters found it. The system was taken as a first orden in a linear range and the results are shown in Figures 35 and 36.

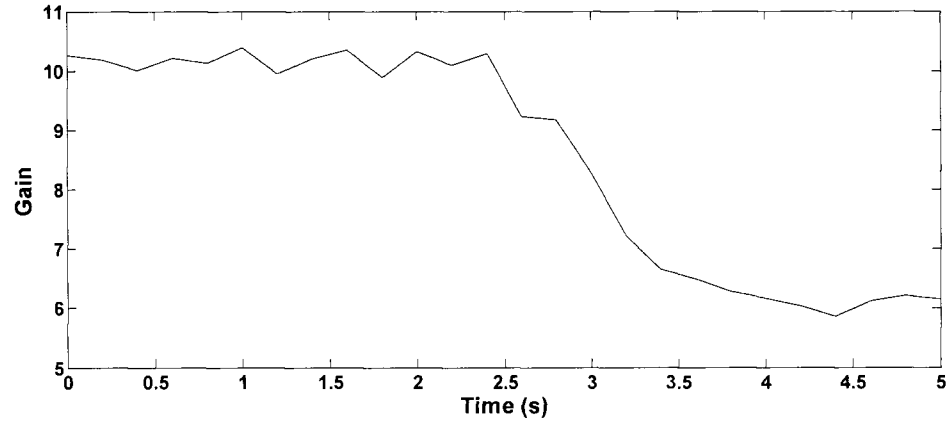


Figure 35. System response for a step change in manipulation in open loop.

The behavior of system in Figure 35 corresponds to the manipulation input in Figure 36.

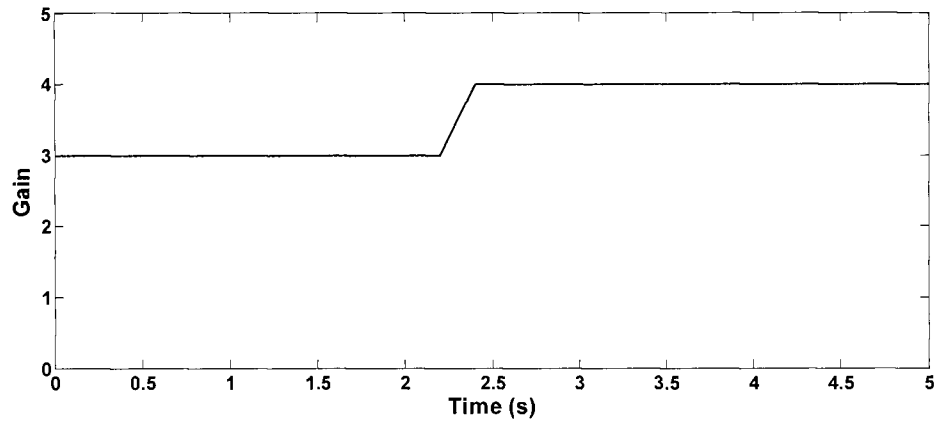


Figure 36. Manipulation step in open loop.

Applying the Ziegler and Nichols method, the parameters for the PI were obtained, but it was necessary to complement by trial and error, in order to improve the tuning, this was done comparing the sum of the squared error (SSE). The recursive equation used for the PI controller was a PID ideal where the derivative parameter is practically zero in this case. The control equation iteration results as follows:

$$u_1 = u_2 + Kc \cdot (e_1 - e_2 + \left(\frac{T}{\tau_i}\right) \cdot e_1 + \left(\frac{\tau_d}{T}\right) \cdot (e_1 - 2 \cdot e_2 + e_3)); \quad (16)$$

where $Kc = -0.5$ and $\tau_i = 0.2$

Figures 37 and 38 show the control response for the PI controller when a perturbation pulse takes place in the system. It can be seen it that the control effort varies around the 3.9 a.u. with a dispersion around 0.6 a.u. (see Figure 37). This variation makes difficult reliable obtaining information from the manipulation control.

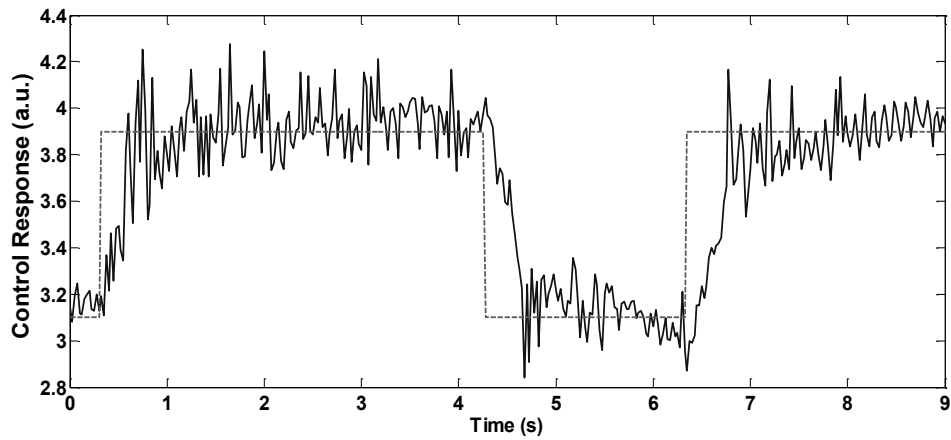


Figure 37. PI control response.

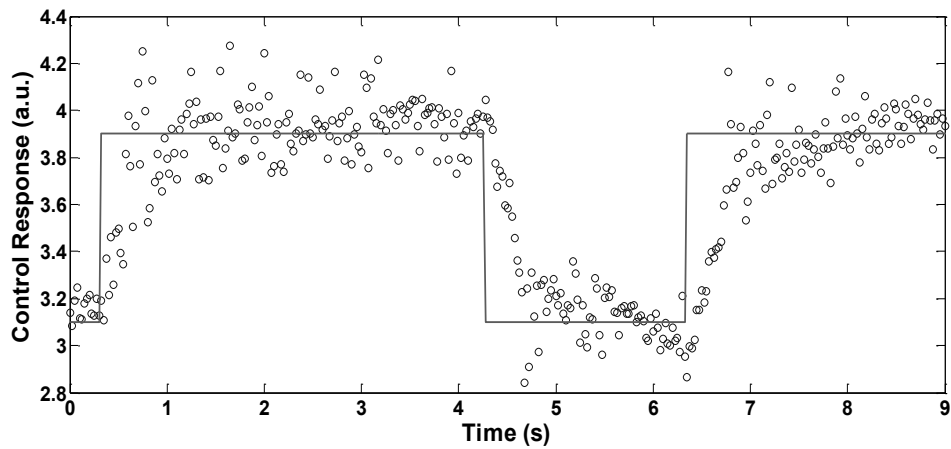


Figure 38. PI control dispersion.

Finally, the SSE was registered from Fuzzy and PI controllers; the same frame time was taken.

Table 2. Sum of Squared error

	SSE
Fuzzy Controller	11.0655939
Proportional-Integral Controller	14.8218329

The above results do not mean that in general the Fuzzy control is better than the PI, but they bring a perspective about the robustness for each one. (Fuzzy and PI control); while the PI needs a model to work, Fuzzy control can regulate the system by logic inferences, and in the particular case of this work, it represents an advantage because the characteristics of the experimentation.

The dispersion shown in Fig. 34 and 38 is due possibly a noise presence. This potential noise effect could be caused by the mechanical coupling and the small signal of the system. Otherwise, the lack of an adequate sampling provided by the DAQ is a serious limitation for this work. Nonetheless, the process variable chosen (rms) is a parameter that can be handle it, because it does not depends directly on the frequency signal, and then, although the sampling rate could have an aliasing effect, if the frequency is not too slow, it is possible reconstruct a similar signal at lower frequency, Certainly the scanning rate cannot be improved but it is possible to experiment in a limit condition, control designs; but definitely is necessary to use another DAQ with a higher frequency performance. The DAQ used in this work is the USB 6001 by National Instruments, and it is focused on academic projects.

4 CONCLUSIONS

4.1. Conclusions.

The following conclusions are derived from this thesis work:

- In order to solve the limitation given by the high frequency on tuning fork, it could be an option to design and produce a particular tuning fork, because the sensitivity of the tuning fork depends on its dimensions.
- Fuzzy control strategy applied to the shear force technique allows representing and reconstructing the topographic information of a sampled surface through the control system consisting of tuning fork, fiber and piezoelectric bimorph as the actuator. So that the nonlinearity does not influence the retrieval of information and its representation through data processing, but it is necessary to find the relation between voltages and distance displacement using optical methods.
- RMS voltage as a measurement variable allows the sensing and control system without the need for a lock-in amplifier.
- To design the fuzzy controller first is necessary to identify the range of operation of the system, not only that, it is also necessary through trial and error to find the actuator operating range, to define the membership functions that will be used , which will be within the range of the actuator previously found.
- In order to obtain an optimum calibration process is necessary, first, to bring the tuning fork (attached to the actuator) a first approximation to the sample surface, then through an external piezoelectric to move the tip until the attenuation zone. The approach can be viewed through a microscope and a laser beam.

4.2. Contribution

The research developed in this thesis contributes to the design of a distance control system based on the technique of shear force, using a tuning fork as a sensing device due to the following contributions:

- The design of a fuzzy controller for a micro-distance control, which can keep the system error near to zero by a control action capable of reconstructing the topographic information of a sample surface. This driver control does not need to know the control system model, only it is enough to know the operating range of the actuator and through experimental tests to define and optimize the control action, providing robustness to the control system and allowing the commercial application through user interface software.
- The electronic instrumentation used in this work provides a reference for developing additional tests to improve and optimize the process of sensing and control, to subsequently develop a practical commercial prototype.

4.3. Future work

The results of this study lay the groundwork for a future commercial development of a device capable of controlling at nanometer-scale the distance between a fiber tip sensing device and a sample surface. This potential application can be used in a microscope SNOM, for the collection of information in nanostructures, topography and composition, as long as the following observations are taken into account:

- It is necessary to characterize the displacement-voltage ratio of the fiber, in order to obtain accurate information of the relief sampled, so it will be possible to make a better calibration of system control and then, improve the accuracy of the controller, necessary for handling small electronic signals.

- The fuzzy controller should be redesigned to improve the performance parameters of the control response, proposing new membership functions and using other fuzzy logic strategies in order to obtain a better control response.
- The signal filtering should be improved by using a data acquisition card with a faster sampling capacity, at least a capacity of 100KHz.
- Having identified the displacement-voltage relationship must be sought sensing techniques to improve the resolution of the control system. Previous works such as Thung *et. al.* [21] propose a solution focusing on the change in the properties of tuning fork, particularly the quality factor, for improving sensitivity and resolution.

5 REFERENCES

- [1] A. Lewis, M. Isaacson, A. Murray and A. Harootunian: J. Biophysics 41, 405a. (1983).
- [2] Pohl, D.W., Denk, W., Lanz, M., App. Phys. Lett. 44, 7 (1984)
- [3] Pohl, D.W., Courjon, D., Near Field optics, Kluwer Academic Publishers. (Netherlands 1993).
- [4] E. Betzig, M. Isaacson, and A. Lewis. Super-resolution fluorescence near-field scanning microscopy. Appl. Phys. Lett. 51, 2088 (1987).
- [5] K. Lieberman, A. Lewis, G. Fish, S. Shalom, T.M. Jovin, A. Schaper, and S. R. Cohen. Multifunctional, micropipette based force cantilevers for scanned probe microscopy. Appl. Phys. Lett. 65. 648-650 (1994).
- [6] E. Betzig, P.L. Finn, and J. S. Weiner. Combined shear force and near-field scanning optical microscopy. Appl. Phys. Lett. 60, 2484 (1992).
- [7] R. Toledo-Crow, P. C. Yang, Y. Chen, and M. Vaez-Iravani. Near-field differential scanning optical microscope with atomic force regulation. Appl. Phys. Lett. 60, 2957 (1992).
- [8] F. Froehlich and T. Milster, Appl. Phys. Lett. 65, 2254 (1994).
- [9] F. Froehlich and T. Milster, Appl. Opt. 34, 7273 (1995).
- [10] B. Hecht, D. W. Pohl, H. Heinzelmann, and L. Novotny, Tunnel near-field optical microscopy: TNOM-2. in *Photons and local probes*, O. Marti and R. Möller, eds. (Kluwer, Dordrecht, The Netherlands) pp.93-107. (1995).
- [11] A. Shchemelinin, M. Rudman, K. Lieberman, and A. Lewis. A simple lateral force sensing technique for near-field micropattern generation. Rev. Sci. Instrum. 64, 3538-3541. (1993).
- [12] J. K. Leong and C. C. Williams, Shear force microscopy with capacitance detection for near-field scanning optical microscopy. Appl. Phys. Lett. 66, 1432 (1995).
- [13] J. Hsu, M. Lee, and B. Deaver, Rec. Sci. Instrum. 66, 3177 (1995).
- [14] J. Barenz, O. Hollricher, and O. Marti, Rev. Sci. Instrum 67, 1912 (1996).
- [15] A. Drabenstedt, J. Wrachtrup, and C. von Borczyskowski, Appl. Phys. Lett 68, 3497 (1996)..
- [16] Karrai K., Grober R. D., Piezoelectric tip-sample distance control for near field optical microscopes. Appl. Phys. Lett. Vol. 66. P.1842-1844 (1995).
- [17] Davis, A., R., Bush, C., Harvey, J. C. and Foley, M. F., "Fresnel lenses in rear projection displays," SID Int. Symp. Digest Tech. Papers 32(1), pp 934-937 (2001).

- [18] Rycken J., Ihn T., Studerus P., Herrmann A., Ensslin K. A low-temperature dynamic mode scanning force microscope operating in high magnetic fields. *Rev. Sci. Instrum.* Vol. 70 pp. 2765-2768 (1999).
- [19] Bruno Ando, Pietro Giannone, Salvatore Graziani, Nicola Pitrone. Measurement system for the characterization of piezoelectric bimorphs. in *Proc. 19th IMEKO TC3*, Cairo, Egypt, Feb. 19-23. (2005).
- [20] R. D. Grober, J. Acimovic, J. Schuck, D. Hessman, P. J. Kindlemann, J. Hespanha, A. S. Morse, K. Karrai, I. Tiemann, and S. Manus, *Rev. Sci. Instrum.* 71, 2776 (2000).
- [21] Vo Than Thung, Chizhik, S.A., Tran Xuan Hoai. Parameters of tip-sample interactions in shear mode using a quartz tuning fork AFM with controllable Q-factor. *Journal of Engineering Physics and Thermophysics.* 82, 1. (2009).
- [22] Karrai, K. Lecture notes on shear and friction force detection with quartz tuning forks. Work presented at the “Ecole Thématique du CNRS” on near-field optics. (2000).
- [23] A. Bouhelier, S. Davy, F. Jeunet, E. Galette, V. Schwartz, M. Spajer, D. Courjon, C. Bainier, P. Blind, and P. Augereau, *Mecatronics* (Universite de Franche-Comte, Besancon, France), Vol. 1, pp. 281–284. (1996).
- [24] Salvi, J.; Chevassus, P.; Mouflard, A.; Davy, S.; Spajer, M.; Courjon, D.; Hjort, K.; Rosengren, L. Piezoelectric shear force detection: A geometry avoiding critical tip/tuning fork gluing. *Review of Scientific Instruments*, Apr98, Vol. 69 Issue 4, pp1744.
- [25] A. Simon, R. Brunner, J. O. White, O. Hollricher, O. Marti (2001). Shear-force distance control at megahertz frequencies for near-field scanning optical microscopy. *2001 Review of Scientific Instruments*, Vol. 72, Issue 11, pp 4178-4182 (2001)
- [26] R. Brunner, A. Bietsch, O. Hollricher, and O. Marti, “Distance Control in Near-Field Optical Microscopy with Piezoelectrical Shear-Force Detection Suitable for Imaging in Liquids,” *Rev. Sci. Instrum.* 68, 1769-1772 (1997).
- [27] R. Brunner, A. Simon, T. Stifter, and O. Marti. Modulated shear-force distance control in near-field scanning optical microscopy. *Review of Scientific Instruments* vol. 71.(1999).
- [28] K. Karrai and R.D. Grober, *Proc. SPIE* 2535, 69 (1995).
- [29] Kevin M. Passino and Stephen Yurkovich, *Fuzzy control* (Addison-Wesley) (1998).
- [30] L. A. Zadeh. Fuzzy Sets. *Informat. Control.* vol. 8 pp.338-353, (1965).
- [31] Dimitar Driankov. *An introduction to fuzzy control*. Springer-Verlag, (1996).

6 APPENDIX A

Appendix A shows the extended literature review.

Leong *et al* [1995].- In this research work it is proposed a non-optical method to detect the shear forces, due to the disadvantage of optical methods like the situation when imaging photosensitive material, it can optically pump the sample. They present an approach using a shear force detection based on a capacitance sensing.

Walid *et al* [1996].- They propose a non-optical phase-locked shear-force microscope using a quartz crystal tuning fork acting as a voltage-controlled oscillator. A tuning fork with a tapered tip is mounted on one of the arms of the fork in a parallel manner. The current through the quartz tuning fork is converted to a voltage and then sent to the feedback circuit. The system scheme is illustrated on Fig. A.1

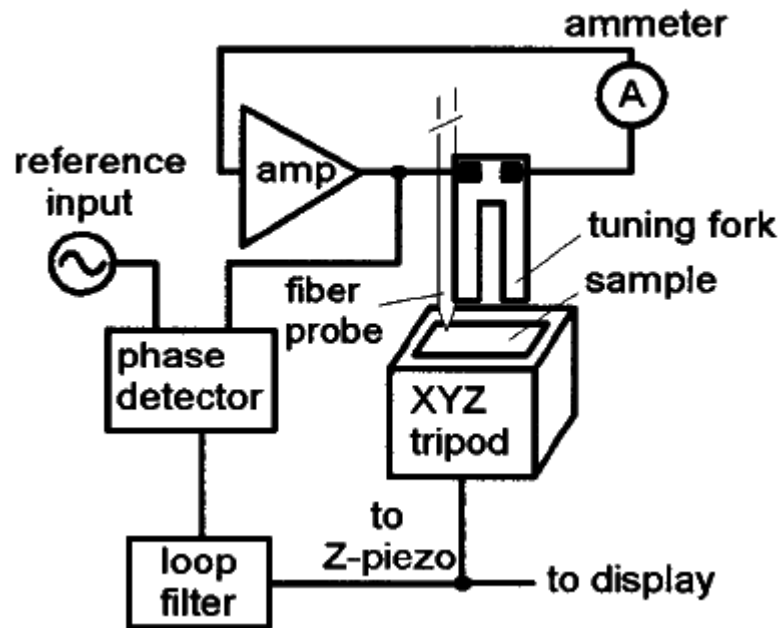


Fig. A.1 Scheme proposed by Leong *et al*.

Salvi *et al* [1997].- The main contribution is an arrangement for mechanical coupling of probe, tuning fork and piezoelectric actuator to detect shear forces without any adhesive between the two prongs of the tuning fork. A proportional controller is mentioned. The proposal is simple and easy to apply. Figure A.2 shows the arrangement proposed by Salvi *et al*.

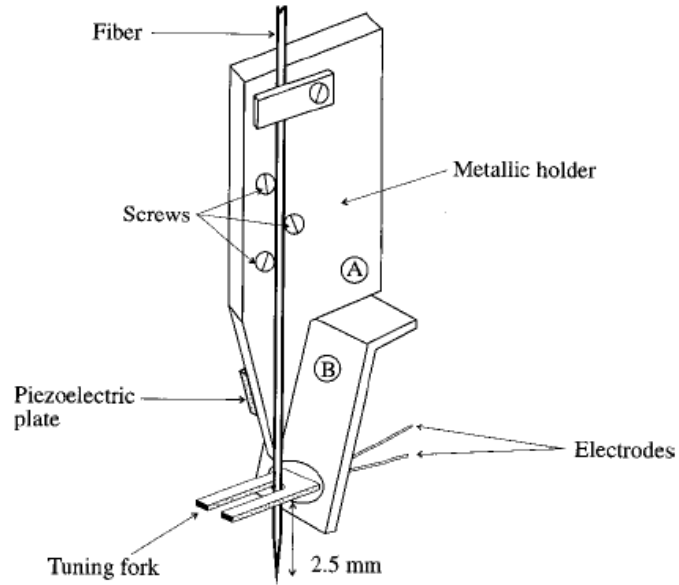


Fig. A.2 Tuning fork and fiber arrangement schematic by Leong *et al*.

Karrai *et al* [1995].- The characteristics of the tuning fork as well as their properties are extensively discussed in this paper. It also suggests an electrical circuit that converts the current into voltage tuning fork for conditioning in the feedback system. As for the mechanical coupling between the fiber and the tuning, it is used a parallel arrangement as it can be seen in Fig. A.3

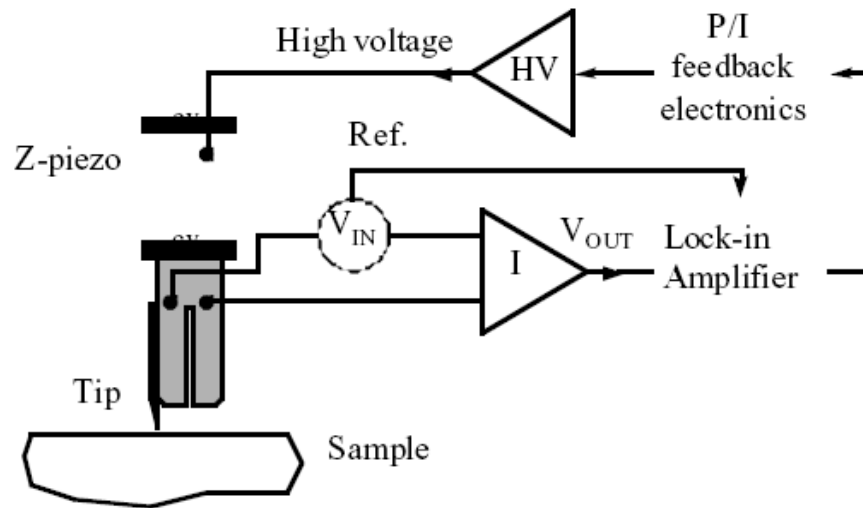


Fig. A.3 Tuning fork and fiber arrangement schematic by Karrai *et al.*

Grober *et al* [1995].- The advantages of using a tuning fork as shear force sensor is explained in this paper. It is a document that examines the characteristics of the piezoelectric and also describes the electronic design used to condition the current to voltage signal from the tuning fork. Paper also mentions the proportional integral control strategy used in experimentation. Fig. A.4 represents the diagram used by Grober.

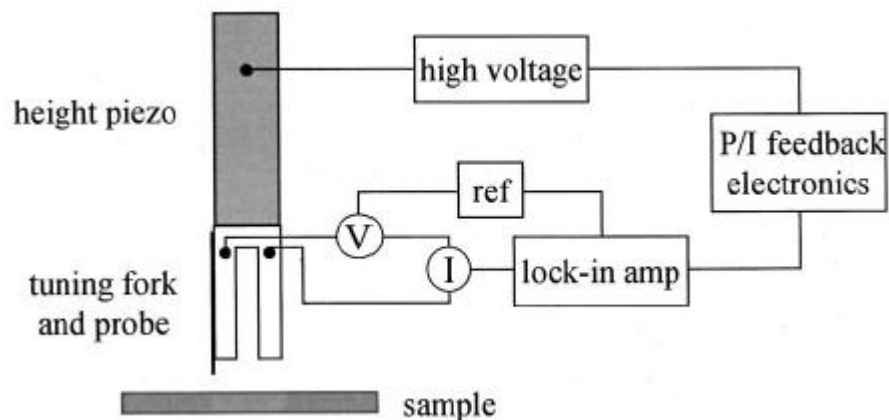


Fig. A.4 Schematic representation of the control system proposed by Grober *et al.*

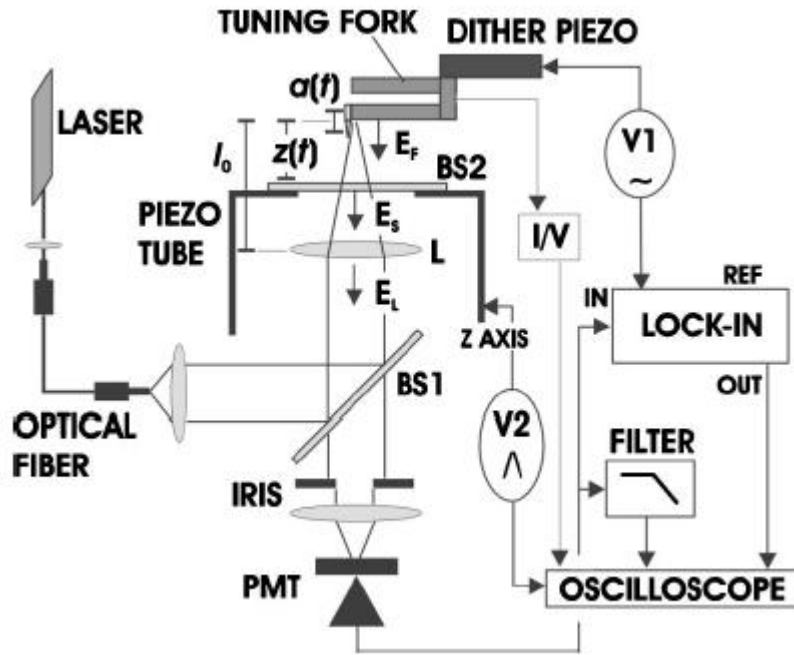


Fig. A.6 Experimental set up utilized by Ohkub *et al.*

Escamilla *et al* [2003].- In this work a fuzzy control strategy is proposed to improve the scanning shear force resolution, instead of modify the quality factor Q in tuning. Moreover a mechanical coupling is implemented, after try with other mechanical configuration.

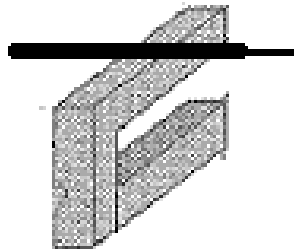


Fig. A.7 Experimental arrangement for tuning fork by Escamilla *et al.*

7 APPENDIX B

In this Appendix the code programmed on Labview by National Instrument is described.

A time loop was included on code, in order to synchronize the sampling rate.

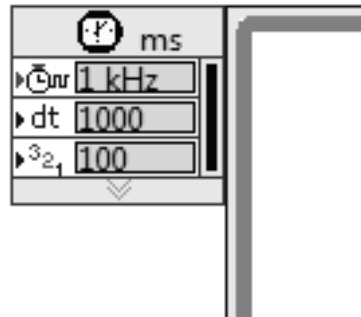


Fig. B.1 Time Loop

The control frame is created as follows:

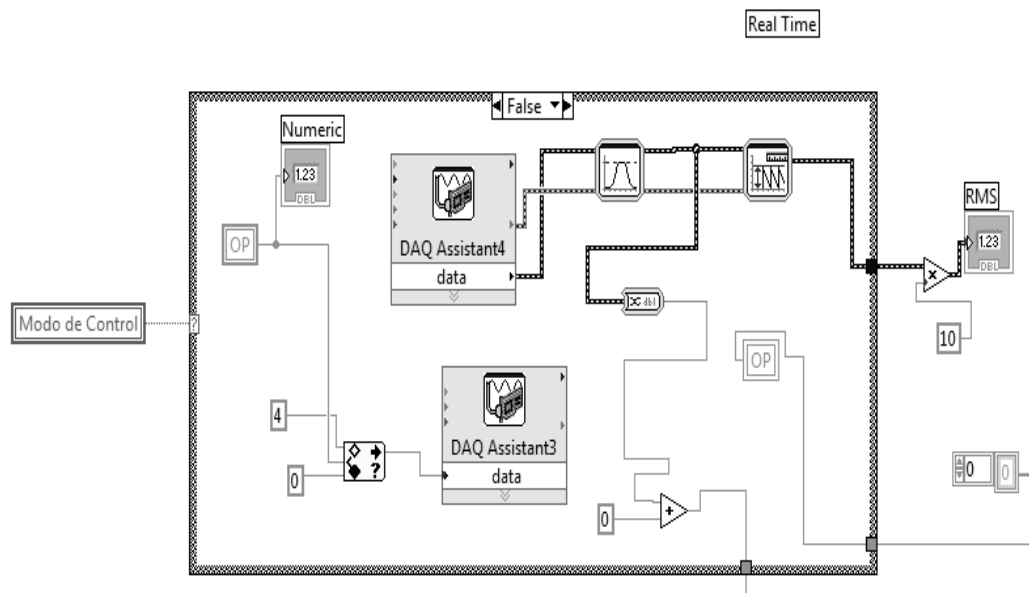


Fig. B.2 Control Frame

For manual or open loop mode control:

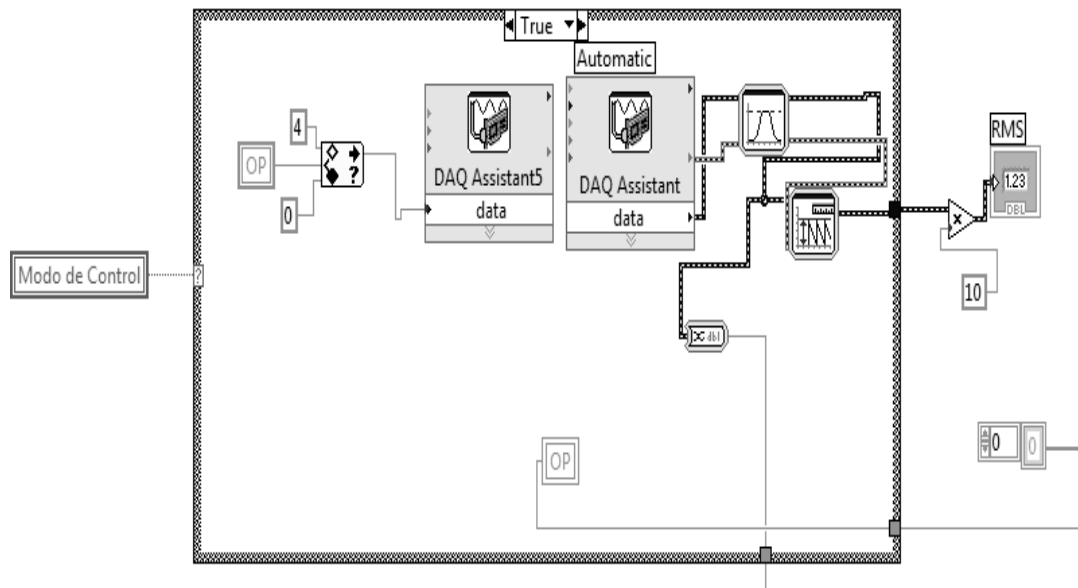


Fig. B.3 Open loop control

The automatic control is defined in Fig. B.2 which is similar to the open loop. A DAQ acquisition toolkit is used to obtain in software the signal sensed from tuning fork. The DAQ has a output range from 0 to 5 volts, so that it is necessary establish a limit, 0-4volts in this particular case. (See Fig. B.4)

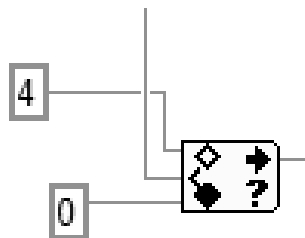


Fig. B.4 Voltage delimiter

In Fig. B.3 there is a RMS block, where the signal generated by tuning fork is detected to identify the RMS value. Fig. B.5 shows the block interface to get the RMS value.

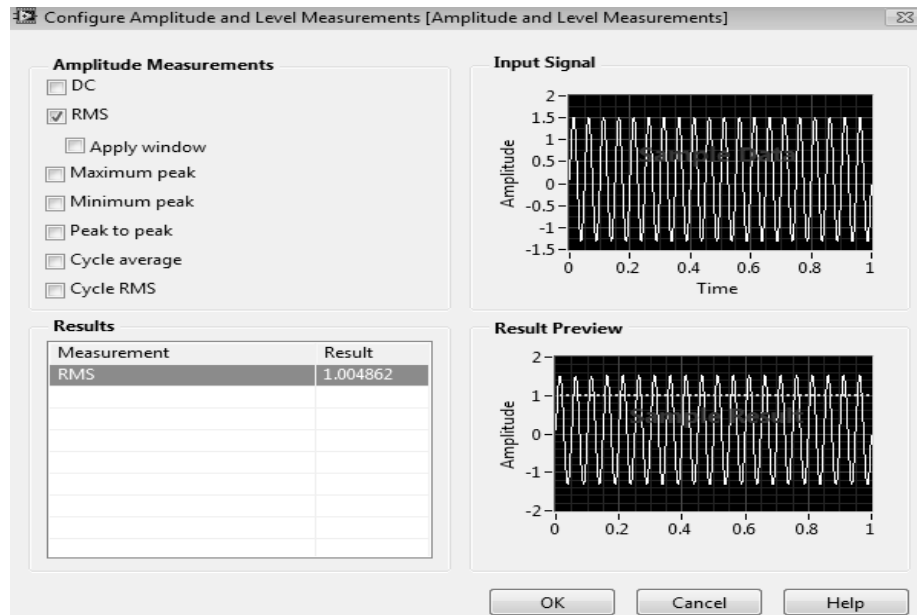


Fig. B.5 Voltage delimiter

The input and output DAQ USB 6008 configuration are illustrated on Fig. B.6 and B.7.

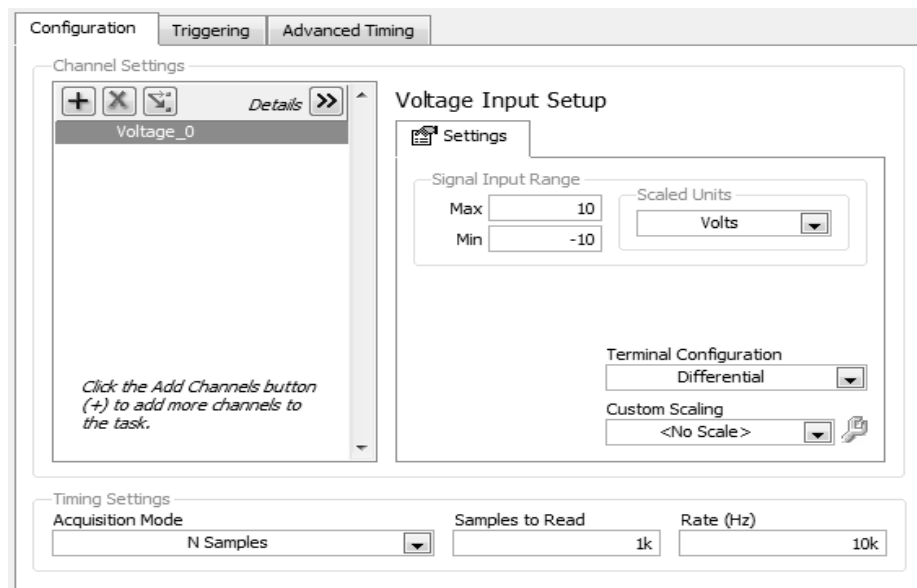


Fig. B.6 Input configuration for DAQ USB 6008

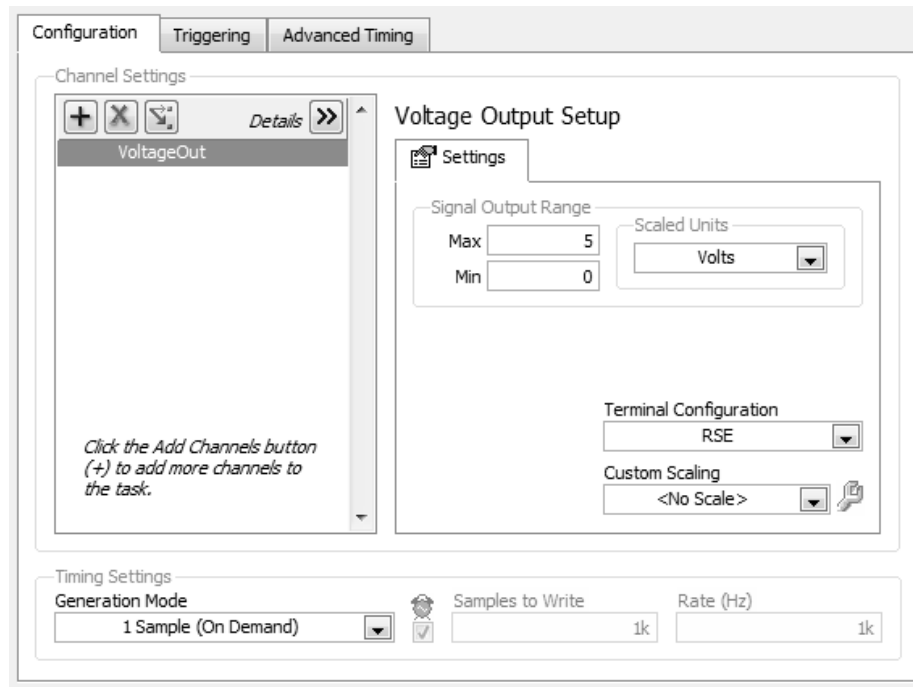
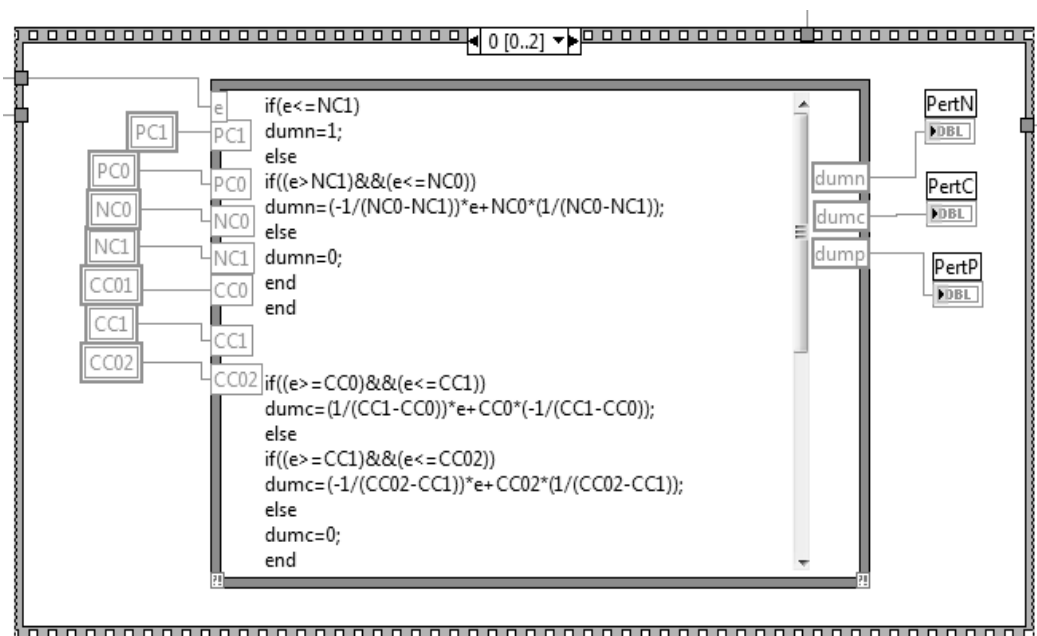


Fig. B.7 Output configuration for DAQ USB 6008

Through a sequence frame the fuzzification error takes place as it is illustrated on Fig. B.8



Fuzzification error derivate:

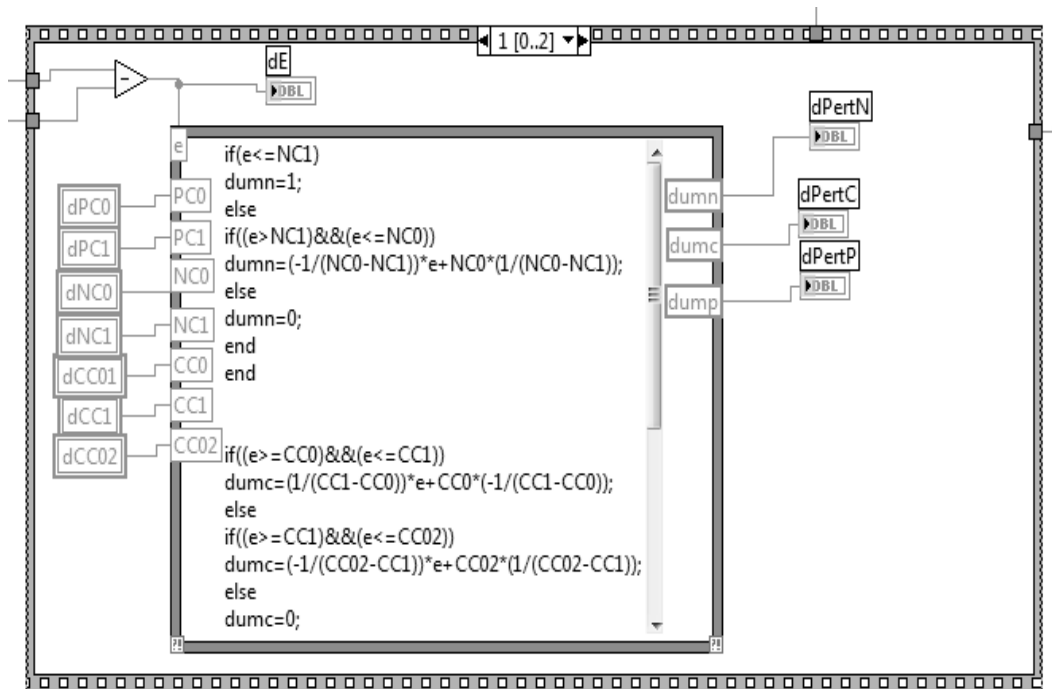


Fig. B.9 Sequence frame for fuzzy controller.

The membership functions are defined by the following Sub-VI's:

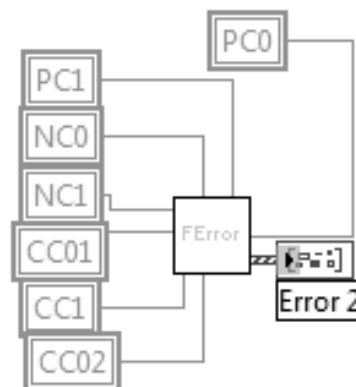


Fig. B.10 Error membership Sub-VI

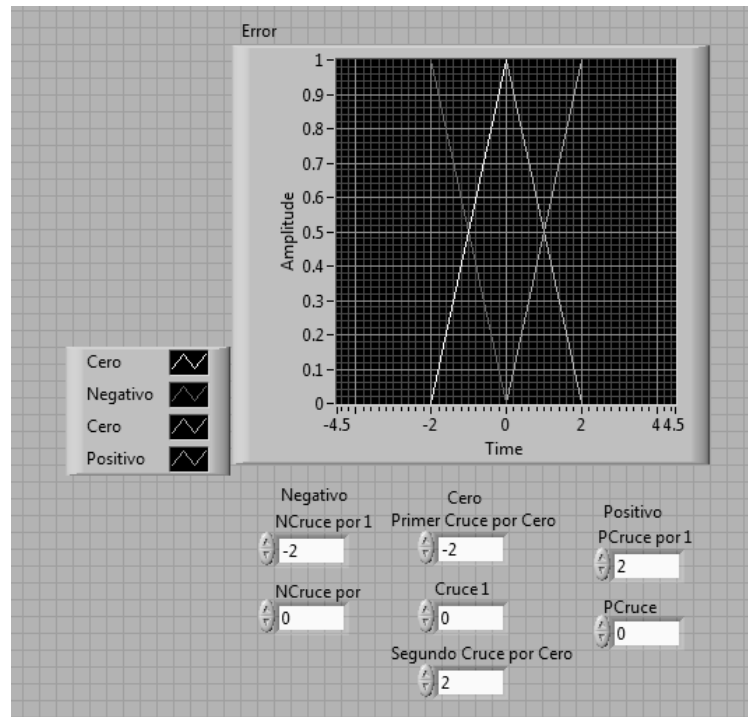


Fig. B.11 Error membership Sub-VI

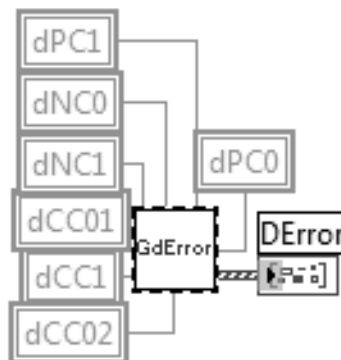


Fig. B.12 Error derivate membership Sub-VI

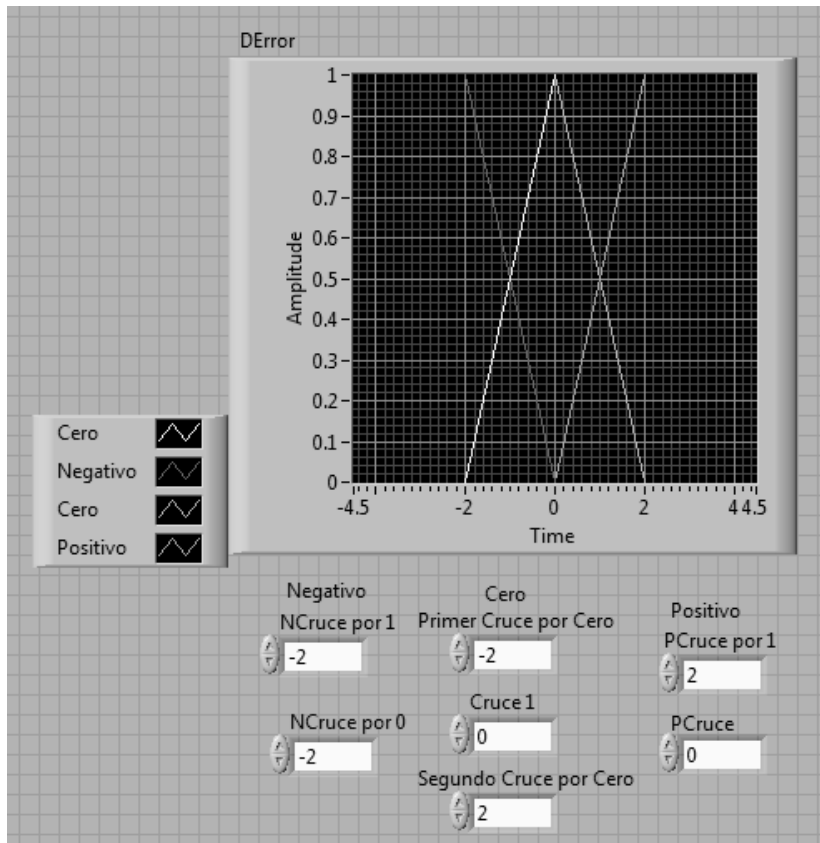


Fig. B.13 Error derivate membership Sub-VI



Fig. B.14 Output membership Sub-VI

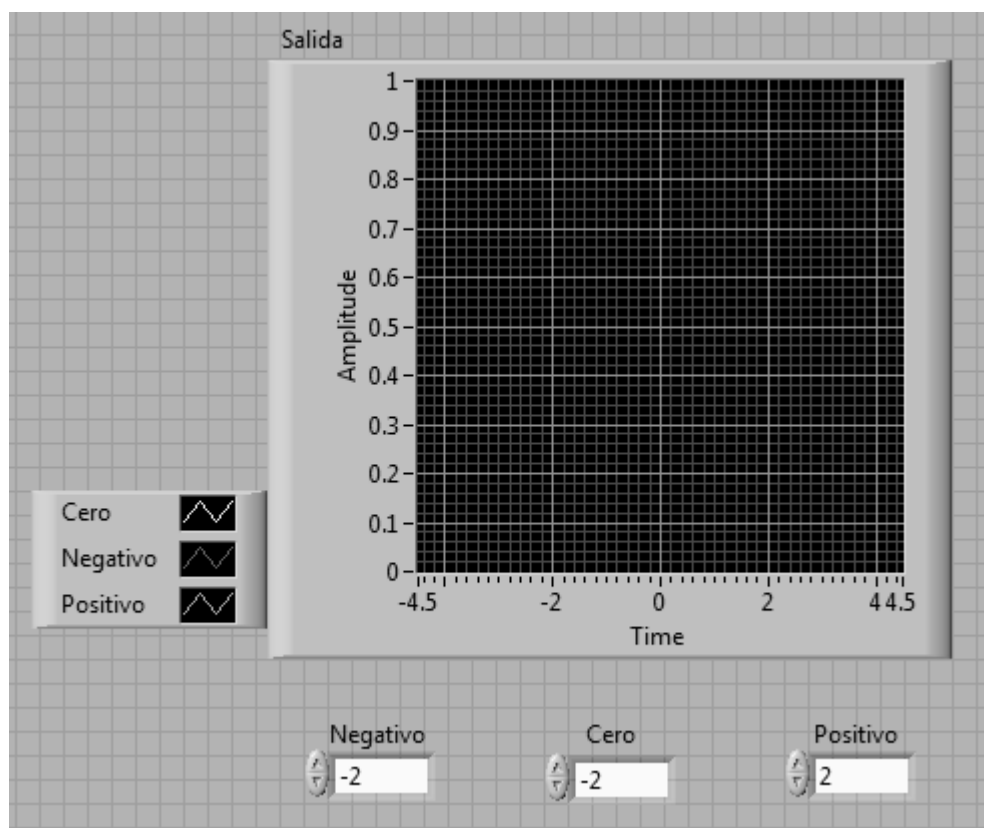


Fig. B.15 Output membership Sub-VI

The defuzzification process for output is making with this labview code:

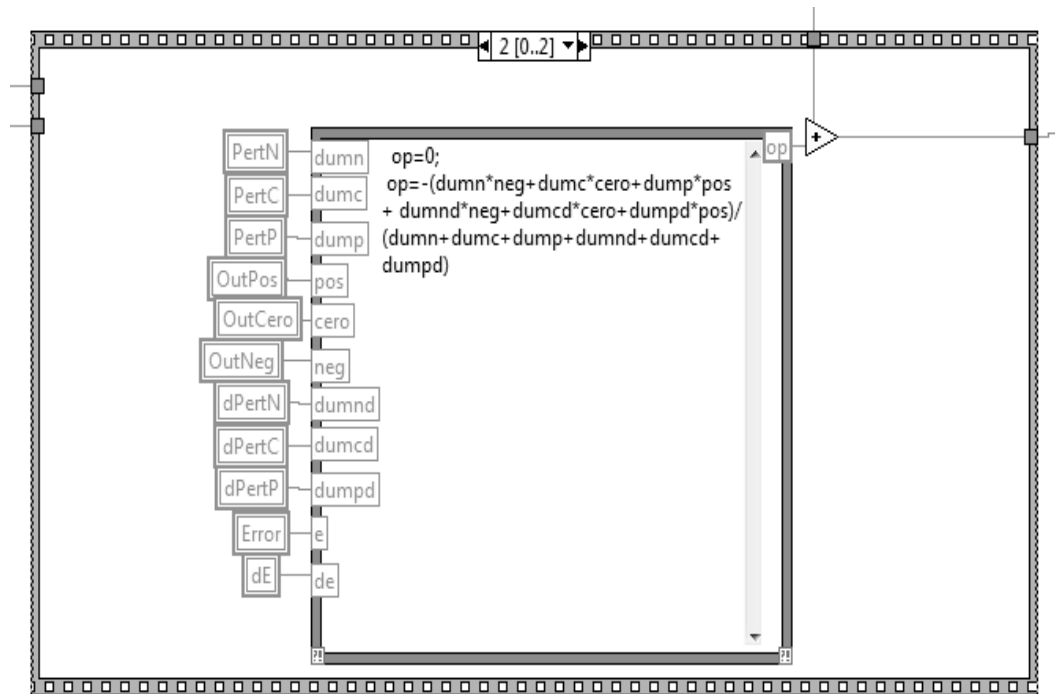


Fig. B.16 Sequence frame for fuzzy controller.

Finally, the file path code:

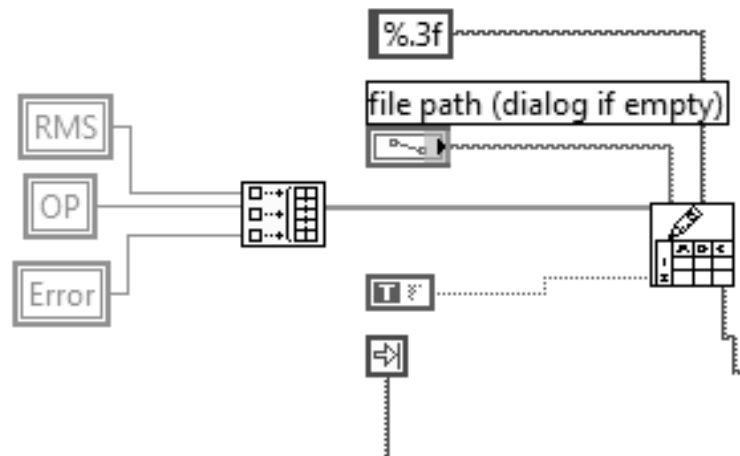


Fig. B.17 File path program